STATE OF CALIFORNIA • DEPARTMENT OF TRANSPORTATION
TECHNICAL REPORT DOCUMENTATION PAGE
DRISI-2011 (REV 10/1998)

Lock Data on Form

1. REPORT NUMBER CA20-3405	2. GOVERNMENT ASSOCIATION NUMBER	3. RECIPIENT'S CATALOG NUMBER
4. TITLE AND SUBTITLE Connected Autonomous Vehicles: Safety During Merging and Lane Change and Impact on Traffic Flow		5. REPORT DATE 09/01/2020
		6. PERFORMING ORGANIZATION CODE University of Southern California
7. AUTHOR Petros Ioannou & Fernando V. Monteiro		8. PERFORMING ORGANIZATION REPORT NO. PSR-18-06 TO-005
9. PERFORMING ORGANIZATION NAME AND ADDRESS University of Southern California 650 Childs Way Los Angeles, CA 90089		10. WORK UNIT NUMBER
		11. CONTRACT OR GRANT NUMBER 65A0674, TASK ORDER TASK ID 3405
12. SPONSORING AGENCY AND ADDRESS California Department of Transportation P.O. Box 942873 Sacramento, CA 94273-0001		13. TYPE OF REPORT AND PERIOD COVERED Final Report, Feb 1, 2019 - April 30, 2020
		14. SPONSORING AGENCY CODE Caltrans

15. SUPPLEMENTARY NOTES

16. ABSTRACT
In this report we address the problem of cooperative lane change maneuvers where vehicles communicate with each other and negotiate the creation of safe spacings in order to merge without taking any safety risks. The proposed approach requires that the merging vehicle negotiates the creation of a safety gap in the destination lane and till the lane change maneuver is completed it operates as having two possible leaders, one in its own lane and one in the destination lane. In addition, the future following vehicle in the destination lane operates as if the merging vehicle has already changed lanes. This approach leads to a smooth creation of spacings for the vehicle to merge into while safety is guaranteed. Furthermore, we expand this solution to platoons of vehicles, develop the communication protocol to be followed, which includes a rule to avoid possible conflicts, and propose measurement verification steps to identify sensor or communication failures. Extensive simulations are used to demonstrate and evaluate the approach under different conditions. They allow us to verify that the proposed control policy generates the desired smooth gap generation behavior. Moreover, we can conclude that the developed methods improve traffic safety and efficiency and reduce environmental impact.

17. KEYWORDS Autonomous vehicles; Connected vehicles; Lane changing; Merging control; Safety; Safety analysis; Traffic flow; Traffic flow rate	18. DISTRIBUTION STATEMENT No Restrictions	
19. SECURITY CLASSIFICATION (of this report) Unclassified	20. NUMBER OF PAGES 60	21. COST OF REPORT CHARGED

Reproduction of completed page authorized.

DISCLAIMER STATEMENT

Connected Autonomous Vehicles: Safety During Merging and Lane Change and Impact on Traffic Flow

Petros Ioannou, University of Southern California
Fernando V. Monteiro, University of Southern California

Contents

Pacific Southwest Region UTC
University Transportation Center

About the Pacific Southwest Region University Transportation Center

The Pacific Southwest Region University Transportation Center (UTC) is the Region 9 University Transportation Center funded under the US Department of Transportation's University Transportation Centers Program. Established in 2016, the Pacific Southwest Region UTC (PSR) is led by the University of Southern California and includes seven partners: Long Beach State University; University of California, Davis; University of California, Irvine; University of California, Los Angeles; University of Hawaii; Northern Arizona University; Pima Community College. The Pacific Southwest Region UTC conducts an integrated, multidisciplinary program of research, education and technology transfer aimed at improving the mobility of people and goods throughout the region. Our program is organized around four themes: 1) technology to address transportation problems and improve mobility; 2) improving mobility for vulnerable populations; 3) Improving resilience and protecting the environment; and 4) managing mobility in high growth areas.

U.S. Department of Transportation (USDOT) Disclaimer

The contents of this report reflect the views of the authors, who are responsible for the facts and the accuracy of the information presented herein. This document is disseminated in the interest of information exchange. The report is funded, partially or entirely, by a grant from the U.S. Department of Transportation's University Transportation Centers Program. However, the U.S. Government assumes no liability for the contents or use thereof.

California Department of Transportation (CALTRANS) Disclaimer

The contents of this report reflect the views of the authors, who are responsible for the facts and the accuracy of the information presented herein. This document is disseminated under the sponsorship of the United States Department of Transportation's University Transportation Centers program, in the interest of information exchange. The U.S. Government and the State of California assume no liability for the contents or use thereof. Nor does the content necessarily reflect the official views or policies of the U.S. Government and the State of California. This report does not constitute a standard, specification, or regulation. This report does not constitute an endorsement by the California Department of Transportation (Caltrans) of any product described herein.

Pacific
Southwest
Region UTC
University Transportation Center

Disclosure

Principal Investigator, Co-Principal Investigators, others, conducted this research titled, "Connected Autonomous Vehicles: Safety During Merging and Lane Change and Impact on Traffic Flow" at Ming Hsieh Department of Electrical Engineering, Viterbi School of Engineering, University of Southern California. The research took place from 2/1/2019 to 4/30/2020 and was funded by a grant from the California Department of Transportation in the amount of $100,000. The research was conducted as part of the Pacific Southwest Region University Transportation Center research program.

Acknowledgements

Pacific Southwest Region UTC
University Transportation Center

Abstract

Despite the recent advancement of autonomous vehicle technology, performing lane changes in dense traffic environments remains an open challenge. One important issue is finding a suitable space to merge without putting either the lane changing vehicle or others in a situation which they cannot handle in case of an emergency. While humans often put themselves at risk for periods of time, autonomous systems must operate as safely as possible at all times without taking any such risks.

In this report we address the problem of cooperative lane change maneuvers where vehicles communicate with each other and negotiate the creation of safe spacings in order to merge without taking any safety risks. The proposed approach requires that the merging vehicle negotiates the creation of a safety gap in the destination lane and till the lane change maneuver is completed it operates as having two possible leaders, one in its own lane and one in the destination lane. In addition, the future following vehicle in the destination lane operates as if the merging vehicle has already changed lanes. This approach leads to a smooth creation of spacings for the vehicle to merge into while safety is guaranteed. Furthermore, we expand this solution to platoons of vehicles, develop the communication protocol to be followed, which includes a rule to avoid possible conflicts, and propose measurement verification steps to identify sensor or communication failures. Extensive simulations are used to demonstrate and evaluate the approach under different conditions. They allow us to verify that the proposed control policy generates the desired smooth gap generation behavior. Moreover, we can conclude that the developed methods improve traffic safety and efficiency and reduce environmental impact.

Connected Autonomous Vehicles: Safety During Merging and Lane Change and Impact on Traffic Flow

Executive Summary

Autonomous vehicles must be able to navigate in vehicle dense environments keeping strict safety guarantees without jeopardizing efficiency. It is particularly hard to obey these objectives during a lane change maneuver, which involves several vehicles and movements in two dimensions. The literature on this subject has already addressed issues spanning from models of human behavior to assessment of maneuver safety and controllers for autonomous lane change. However, procedures to deal with situations where the current state of surrounding vehicles does not satisfy minimum safe conditions are still lacking. We tackle this issue by making use of vehicle connectivity to generate the necessary spacings efficiently. We first investigate safe lane change space definitions and come up with a simplified conservative estimation. This estimate not only takes into account vehicle parameters and current traffic state but is also easily integrated in vehicle following controllers. Then, we address the communication protocol, defining the steps a vehicle must follow from requesting a gap at the desired destination lane until moving into it. Within this framework, we propose using maneuver priority levels to manage conflicts. After that, the use of connectivity leads our focus to maneuvers of vehicle platoons. We not only extend previous results on the minimum safety gaps requirements but also introduce three strategies that allow the whole platoon to perform the maneuver together. They are: Synchronous, Leader First and Last Vehicle First. Next, we turn our attention to another level of safety by studying ways of mitigating possible sensor or communication issues. A verification protocol which compares sensor and communication measurements to internal model predictions is suggested to identify faults. Following a consistency check, an analysis of fault severity determines in which cases the driver is required to take control. After having set the basis for strict safety guarantees, we develop an approach capable of generating the desired behavior in an efficient manner. The vehicle which wants to change lanes adjusts its longitudinal position based both on the preceding vehicle on the same lane and on the vehicle behind which it intends to merge. This is called virtual vehicle following and it ensures safety while positioning the vehicle at the proper place for the maneuver. Simultaneously, the future follower smoothly creates the safe space for the incoming vehicle by adopting the lane changing vehicle as its virtual leader. Besides the theoretical guarantees, we perform extensive simulations to corroborate our claims. A detailed implementation of the controllers in Simulink allows to verify the desired behavior in well-defined scenarios. Moreover, we extract metrics to evaluate the performance of the different platoon strategies under varied traffic conditions. Last, we assess the traffic and environmental impact on a larger scale using the microscopic simulator VISSIM. The results indicate that the proposed methods improve safety and efficiency on highway travels.

Pacific Southwest Region UTC
University Transportation Center

1 Introduction

The need for more efficient safer vehicles is self-evident: congestion costs were estimated above
US$87 billion in 2018 [1] and there were almost 35,000 fatalities in 2017 in the United States alone
[2]. One promising way of alleviating these issues is through autonomous vehicles [3, 4]. While
some driving tasks, such as Adaptive Cruise Control (ACC) [5, 6] are already well understood
enough to be integrated in commercial vehicles, others still require more study and evaluation.
One of these more complicated tasks is lane changing. It is one of the most stressful maneuvers
that a driver must perform since it involves changes in longitudinal and lateral velocities while
keeping track of relative positions and velocities of several surrounding vehicles. According to
the survey in [7], lane changes are responsible for one tenth of all accidents, cause congestion
at lane drop locations and act as "moving obstacles", which leads to decreased freeway capacity.
Therefore, there is a continuous effort to automate this maneuver.

While there are studies to evaluate lane change feasibility [8–10] and others to determine how
to make use of the existing space [11, 12], generating the necessary gaps when these do not exist is
still an open challenge in the field. A motivating example is the situation of merging into a highway
with heavy traffic. In this case, an autonomous vehicle may never find a suitable safe gap. De-
pending on the highway design, this would force the vehicle to either block all traffic on the access
ramp or to stay at the acceleration lane until the next highway exit. While humans drivers can deal
with this type of situation by putting themselves at risk, driving algorithms must be designed to
avoid prone-to-collision situations. In addition, the advancements in vehicle connectivity give rise
to vehicle platoons which are able to increase road throughput thanks to small inter-vehicle fol-
lowing distance [3, 13]. The side effect noted in [14] is that such small gaps make finding suitable
lane change spacings more challenging.

The main goal of this project is to propose solutions that rely on Connected Autonomous Ve-
hicles (CAVs) to guarantee safety and feasibility of lane changes in vehicle dense traffic scenarios.
Our efforts are focused on the tactical and operational stages of lane changes, which means we
assume the decision to perform the maneuver is given by a higher level decision algorithm. We
address the issues of:

1. Feasibility: given the current traffic state, find out if it is safe to start a lane change. If not,
   determine what is the minimum safe gap;

2. Communication: make use of connectivity to determine feasibility and how to proceed if
   safe gaps are not available.

3. Platooning: adapt the feasibility checks and the communication strategy when entire pla-
   toons of vehicles decide to change lanes;

4. Gap verification: leverage sensors, communication and analytical redundancy to verify the
   existence of safe gaps;

5. Efficiency: design strategies and controllers that minimize the impact on traffic while guar-
   anteeing safety;

**Pacific
Southwest
Region UTC**
University Transportation Center

6. Evaluation: demonstrate through simulation the effects of all proposed methods.

After a literature review of the relevant topics in section 2, sections 3 through 8 of this report discuss the above subjects in the given order. Section 9 summarizes the main findings.

2 Literature Review

Given the importance of lane change maneuvers highlighted in the Introduction, the continuously growing literature on the subject comes as no surprise. Studies range from attempts to model human behavior [15–17] to controllers capable of performing lane-changes autonomously [11,18]. With a focus on determining maneuver safety, the work in [8] uses a sinusoidal lateral acceleration model alongside constant speed assumptions to compute longitudinal safe gaps between an ego vehicle and the surrounding vehicles before starting the lane change. Then, in [9], situations where there is emergency braking during the lateral movement are studied. These results are used in [19] to analyze safety of platoon maneuvers and determine whether inter-vehicle spacing should increase before all vehicles start lane changing. More recently, works [10] and [20] build upon the results from [8] to propose safe multivehicle lane change planning. A different approach is taken in [21], where, instead of measuring and checking for safe gaps, vehicles consider a maneuver to be safe based on the deceleration they will force on their future follower. Still dealing with maneuver feasibility, perception uncertainty is explicitly included in [22] and [23], whereas [12] uses game theory to estimate other vehicles' reactions and decide when lane changing is safe. From a different perspective, [24] defines a risk level measure to determine the risk of a lane change and uses real world datasets to analyze how human driving relates to that measure. Addressing a related issue, the authors of [25] deal with how to place the vehicle at the appropriate longitudinal position for lane change by solving a quadratic optimization problem with constraints on vehicle position, velocity, acceleration and jerk.

Thanks to standards such as Dedicated Short-Range Communications (DSRC) [26], properly equipped vehicles can communicate either to other vehicles (V2V) or to the infrastructure (V2I) and results from [27] indicate that DSRC's reliability is adequate for communications during lane change. At this point, it is important to differentiate passive from active cooperation. In the former, cooperation is a synonym of communication: the only cooperative action vehicles perform is to share information that others cannot gather from their own sensors. For example, in [18] vehicles use V2V to obtain information about surrounding vehicles and construct artificial potential fields that guide their movement. Differently, in active cooperation, CAVs are expected to alter their behavior to achieve system level goals, such as safety or improved efficiency. Due to the insufficient spacings, lane changing in congested situations requires active cooperation. This idea was first applied in cooperative merging [28], where highway vehicles make space for on-ramp incomers. Despite the success of these methods, they cannot be directly applied to the more general case of lane changes due to the fact that merging must occur within a predefined area. This constraint often yields procedures that depend on the existence of a roadside unit which can communicate to vehicles, perform a centralized optimization and determine the merging order [18]. The main idea we borrow from this domain, as will be seen later, is the one of virtual vehicles [29, 30], which al-

lows a vehicle to adjust its longitudinal speed and position based on a vehicle traveling on another lane.

When it comes to creating large enough gaps for lane changes, [31] applies an LQR controller specifically to generate bigger spacings. With another approach, the authors of [32] just change the setpoint of the constant time headway controller already in place and successfully test their algorithm in real vehicles. However, neither approach addresses how to keep the lane changing vehicle at the proper position to initiate the maneuver. This is partially addressed in [33], where VISSIM is used to simulate a scenario in which an accident forces vehicles to change lanes. The paper proposes an algorithm that not only requests vehicles on adjacent lanes to brake in order to create the necessary gaps, but also computes desired speeds for the merging vehicles. While improved throughput in simulations validates the method's usefulness, the gap generating controller works by computing vehicles' speeds, which cannot be directly controlled in practice. Furthermore, there are no proofs that spacings are successfully created for every request. Differently, the work in [34] adopts a nonlinear longitudinal controller derived from well tuned artificial potential fields. When a vehicle has the intention to change lanes, the artificial potential fields in its own controller as well as the ones in the gap generating vehicle are modified in a way which ensures that all vehicles are at safe distances from each other before the maneuver starts. To prove the controllers always yield safe behavior, the authors have to make some restrictive assumptions. First, they consider that the lane changing vehicle has no one in front of it, which is not true in congested scenarios. Second, they expect the future leader to be always longitudinally ahead and faster than the lane changing vehicle. This assumption is violated if the future leader is forced to brake abruptly. In [35] the ACC stems from an optimal control problem whose costs includes factors for safety, efficiency, and comfort. By finding optimal acceleration inputs for different lanes and computing the respective costs, vehicles decide whether to move from their current lane. The paper is not directed at cooperation for gap generation, but this behavior can be observed if vehicles include the costs of others when optimizing their own trajectory. To reduce the computational burden, lane changes can only be performed at predetermined fixed time instants and the optimization problem has no constraints on control inputs or vehicle states. Therefore, to guarantee safety and feasibility of solutions, the cost functions weights must be finely tuned. The demanding task of lane change within platoons is analyzed in [36]. The approach requires that platoon leaders communicate to allow a vehicle to move from one platoon to the other. Given the open-loop nature of the gap generation procedure and the need for platoons to be aligned, unexpected behavior of downstream vehicles might prevent the creation of proper spacings.

3 Safety Spacing Requirements

This section discusses how to determine the minimum safe distances between each of the vehicles involved in the lane change maneuver. To do that, the ego vehicle E, which is planning to perform the maneuver, must consider a few factors. The first one is that a safe vehicle following distance to vehicles on the same lane must be maintained till the lane change maneuver is completed. The second is a transient gap, which takes care of the relative distance variation during the maneuver
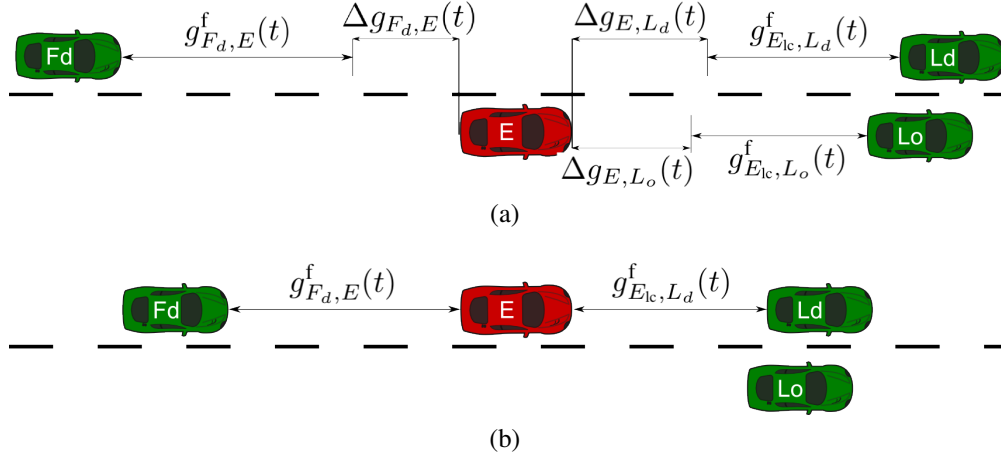
Figure 1: In (a), minimum safe lane change gaps that must be created before the maneuver can start. In (b), expected distances right after the maneuver is completed.

while considering both longitudinal and lateral positions. The final factor is that, during the lane change, E's braking capability decreases. We also note that E must guarantee large enough distances to three of its surrounding vehicles, namely: leader in the destination lane (L_d), follower in the destination lane (F_d), and leader in the original lane (L_o). The distance to the follower in the original lane (F_o) is not addressed, since this vehicle is assumed have its own safe vehicle following controller. These ideas are summarized by Fig. 1, where $g_{i,j}^{\mathrm{f}}(t)$ is the safe vehicle following distance between vehicles i and j at time t and $\Delta g_{i,j}(t)$ is the transient gap. The rest of this section details how to compute the safe spacings and presents numerical results of the proposed methods.

3.1.   Safety Spacing in Vehicle Following

Safe vehicle following can be defined as keeping a sufficient distance from a leading vehicle that is in same lane as the ego vehicle such that, if the lead vehicle stops in an emergency, the ego vehicle can also do so without any collision. To compute the minimum safe distance, let's start by defining the gap between the ego vehicle E and its leader L:

$$g_{E,L}(t) = (x_L(t) - l_L) - x_E(t), \tag{1}$$

where l_i is the length of vehicle i, $i \in \{E, L\}$, and $x_i(t)$ is the longitudinal position of its front bumper at time t. The gap evolves over time as:

$$g_{E,L}(t) = g_{E,L}(t_0) + (v_L(t_0) - v_E(t_0))t + \int_{t_0}^{t} \int_{t_0}^{\lambda} (a_L(\tau) - a_E(\tau)) \mathrm{d}\tau \mathrm{d}\lambda. \tag{2}$$

where $v_i(t)$ and $a_i(t)$ are vehicle i's longitudinal velocity and acceleration respectively, and t_0 is the initial time. To guarantee safety in an emergency braking scenario, we need $g_{E,L}(t) \geq 0$ for
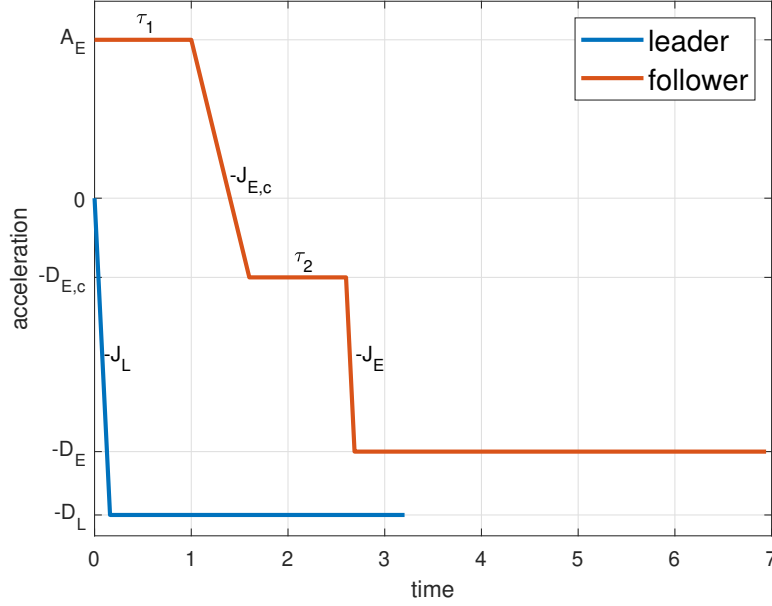
Figure 2: Acceleration profiles for the leader and follower.

$t_0 \leq t \leq T$, where t_0 takes the value of the time instant when the leader starts braking and T is the
time when both vehicles achieve full stop. Therefore, the minimum safe gap is:

$$g_{E,L}(t_0) \geq (v_E(t_0) - v_L(t_0))t + \int_{t_0}^{t} \int_{t_0}^{\lambda} (a_E(\tau) - a_L(\tau)) \mathrm{d}\tau \mathrm{d}\lambda, \quad \forall t \in \mathbb{T}$$

$$g_{E,L}^*(t_0) = \max_{t \in \mathbb{T}} \left[(v_E(t_0) - v_L(t_0))t + + \int_{t_0}^{t} \int_{t_0}^{\lambda} (a_E(\tau) - a_L(\tau)) \mathrm{d}\tau \mathrm{d}\lambda \right], \qquad (3)$$

where $\mathbb{T} = [t_0, T]$. To compute values for $g_{E,L}^*(t_0)$, we need to define the leader's emergency brak-
ing behavior and E's reaction to that. Concerning the former, the most conservative case, known
as "brick wall" [37, 38], assumes that the leader stops instantaneously. This assumption leads to
impractically large distances. In [37] and [6], the leader is assumed to have zero acceleration at t_0,
apply maximum negative jerk until reaching maximum deceleration $-D_L$ and then keep this de-
celeration until full stop. The ego vehicle is assumed to have maximum acceleration A_E at t_0. This
can be viewed as a situation where E is trying to "catch-up" with L. After a delay τ_1, E realizes its
leader is braking. However, at first, the ego vehicle does not know this is an emergency situation
and applies a comfortable negative jerk $-J_{E,c}$ until it reaches a comfortable deceleration $-D_{E,c}$.
After a second delay τ_2, E notices that this is an emergency scenario. By then, it brakes with max-
imum jerk $-J_E$ until it reaches a maximum deceleration $-D_E$. Finally, it keeps this deceleration
until full stop. The whole process is summarized by Fig. 2. The authors of [6] vary the delay
values τ_1 and τ_2 to model three classes of drivers: human, autonomous and connected. The first
has both delay values larger than the second, while the connected vehicle skips the comfortable
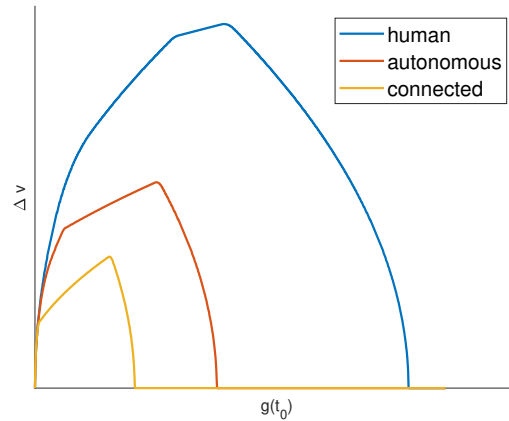
Figure 3: Severity as a function of the initial gap for the different driver types described in [6].

braking phase and goes straight into emergency braking after a single delay.

If, $g_{E,L}(t_0) < g^*_{E,L}(t_0)$, collision severity can be estimated by a measure called Delta-V [39], which describes the absolute difference in vehicle speed before and after a crash. Under the assumption of inelastic collision:

$$\Delta v_E = \frac{m_L}{m_E + m_L} \left(v_E(t_-) - v_L(t_-) \right), \tag{4}$$

where m_i is the mass of vehicle i and $v_i(t_-)$ is the velocity of vehicle i right before collision. Assuming vehicles of equal mass, severity is plotted against initial gap for the three classes of driver in Fig. 3. The advantages of CAVs become evident: it is possible to have considerably smaller inter vehicle gaps, which increase road capacity, without compromising safety.

In what follows, we assume that vehicles are connected, so E goes straight into emergency braking after a delay τ, and that $D_L \geq D_E$, which means the leader is able to brake at least as hard as the ego vehicle. This yields the closed form solution for Eq. (3):

$$g^*_{E,L}(t_0) = \frac{v_E^2(t_0)}{2D_E} - \frac{v_L^2(t_0)}{2D_L} + \lambda_1 v_E + \lambda_2 \tag{5}$$

where:

$$\lambda_1 = \tau + \frac{A_E + D_E}{J_E} + \frac{1}{D_E} \left(A_E \tau + \frac{A_E(A_E + D_E)}{J_E} - \frac{(A_E + D_E)^2}{2J_E} \right) \tag{6}$$

and

$$\lambda_2 = \frac{1}{2} A_E \tau^2 + \frac{A_E (A_E + D_E)^2}{2 J_E^2} - \frac{(A_E + D_E)^3}{6 J_E^2} + \frac{A_E (A_E + D_E)}{J_E} \tau + \frac{1}{2 D_E} \left(A_E \tau + \frac{A_E (A_E + D_E)}{J_E} - \frac{(A_E + D_E)^2}{2 J_E} \right)^2 .$$

(7)

Variables λ_1 and λ_2 are measured in seconds and meters respectively and their computation is detailed in [5]. Setting $D_E = \gamma D_L$, where $0 < \gamma \leq 1$, describes the more limited braking of the ego vehicle. Trucks following passenger vehicles, for example, should adopt low values of γ. Moreover, let $v_L(t_0) = \rho v_E(t_0)$, where $0 < \rho \leq 1$, in order to account for possible velocity differences. This yields:

$$g_{E,L}^*(t_0) = \left(\frac{1 - \gamma \rho^2}{2 D_E} v_E(t_0) + \lambda_1 \right) v_E(t_0) + \lambda_2.$$

(8)

It should be noted that setting either γ or ρ equal to zero is equivalent to the "brick wall" scenario. We can define:

$$h = \frac{1 - \gamma \rho^2}{2 D_E} \bar{v}_E + \lambda_1,$$

(9)

where $\bar{v}_E$ is an upper limit on E's velocity, such as the road's maximum speed or the desired traveling velocity. While the relationship of h to D_E remains non-linear due to λ_1, the sensitivity with regard to the difference in braking capabilities and initial speeds is clear. This leads to a safe vehicle following distance known as constant time headway policy, which is seen often in the Adaptive Cruise Control Literature [5, 40] and is used throughout this work:

$$g_{E,L}^f(t_0) = h v_E(t_0) + d_0,$$

(10)

where h is usually called the time headway, and d_0 is the desired distance at standstill. For simplicity, we choose $d_0 = \lambda_2$.

3.2.   Transient Lane Change Gap

Before a lane change, velocities of E, F_d and L_d can differ considerably and it is desirable to avoid large acceleration or deceleration while performing the lateral adjustment. Therefore, it is necessary to take into account the longitudinal distance variation during the maneuver. This ensures that, despite non-zero relative velocities between E and the surrounding vehicles, the lane change starts and ends respecting safe vehicle following distances. To achieve this, we follow the approach from [8]. First, let E's lateral acceleration be modeled as:

$$a_y(t) = \begin{cases} \frac{2\pi H}{\Delta t_{lc}^2} \sin \left(\frac{2\pi}{\Delta t_{lc}} (t - t_{adj}) \right), & t_{adj} \leq t \leq t_{lc} \\ 0, & \text{otherwise,} \end{cases}$$

(11)

where H is the total lateral displacement, t_{adj} is the time instant after longitudinal adjustments, t_{lc} is the time instant after the lane change is completed and $\Delta t_{\text{lc}} = t_{\text{lc}} - t_{\text{adj}}$ is the lane change duration. The equation above is used to determine the time intervals $\mathbb{T}_k = [t_k, T_k]$ in which the lateral coordinates indicate that a collision between E and $k \in \{L_d, F_d, L_o\}$ is possible. The obtained solution for relative distance variation during lane change is similar to Eq. (3) changing $\mathbb{T}$ by $\mathbb{T}_k$.

Because we demand safe vehicle following distances to be respected at the start and end of the lane change, we only need to consider $t_k \geq t_{\text{adj}}$ and $T_k \leq t_{\text{lc}}$, $\forall k$. Furthermore, we assume all vehicles keep constant speed during lane change. The method to guarantee this strong assumption holds is presented further on in section 7. Thus, the gap variation during lane change to the leaders is:

$$\Delta g_{E,k}(t_{\text{adj}}) = \max_{t \in \mathbb{T}_k} \left[(v_E(t_{\text{adj}}) - v_k(t_{\text{adj}})) \, t \right], \tag{12}$$

where $k = \{L_o, L_d\}$ and to the future follower is:

$$\Delta g_{F_d,E}(t_{\text{adj}}) = \max_{t \in \mathbb{T}_{F_d}} \left[(v_{F_d}(t_{\text{adj}}) - v_E(t_{\text{adj}})) \, t \right]. \tag{13}$$

3.3.   Safety Spacing for Lane Change

Finally, one must account for the possibility of braking during the lane change. It is well known that, when the vehicle's wheels form a non-zero angle with its moving direction, its braking capabilities are reduced. This idea, expressed by the friction circle [40], can be described by

$$a_x^2 + a_y^2 = C \tag{14}$$

where a_x and a_y are the vehicle's longitudinal and lateral acceleration respectively, and C is a positive constant related to tire friction. It should be noted that the above equation is only valid when braking happens during lateral movement. For pure longitudinal braking the maximum longitudinal acceleration is not constrained to $\sqrt{C}$. The authors of [9] use this equation to develop an algorithm that computes safe distances by considering all possible initial braking times. We adopt a simpler, more conservative approach which allows the vehicle to keep using a time headway based distance. It is derived as follows. Starting from Eq. (11), it is possible to obtain the maximum lateral acceleration $A_y = 2\pi H/\Delta t_{\text{lc}}^2$, use it in the friction circle equation and compute the minimum maximum longitudinal braking during lane change:

$$D_{E,\text{lc}}^2 = C - A_y^2. \tag{15}$$

By construction, $D_{E,\text{lc}} < D_E$, which yields larger values for the safety vehicle following spacing. To get the values of h_{lc} and $d_{0,\text{lc}}$, we use both $D_{E,\text{lc}}$ and a new value $A_{E,\text{lc}}$ based on the expected acceleration at the beginning of the maneuver. This implies E has to increase its distance to L_o before starting the maneuver. Finally, the safe gaps for lane changing are a sum of the safe vehicle

Table 1: Vehicle parameters.

Parameter [unit]	Passenger Vehicle	Truck
mass $[kg]$	2000	18000
length $[m]$	5	18
width $[m]$	1.8	2.4
$A_{\max}[m/s^2]$	4	2
$-D_{\max}[m/s^2]$	-8	-3
$|J_{\max}|[m/s^3]$	50	30
$\delta[s]$	0.3	0.3

following distance and the transient gaps:

$$g^{\text{lc}}_{E,L_o}(t_{\text{adj}}) = g^{\text{f}}_{E_{lc},L_o}(t_{\text{adj}}) + \Delta g_{E,L_o}(t_{\text{adj}}), \qquad (16)$$

$$g^{\text{lc}}_{E,L_d}(t_{\text{adj}}) = g^{\text{f}}_{E_{lc},L_d}(t_{\text{lc}}) + \Delta g_{E,L_d}(t_{\text{adj}}), \qquad (17)$$

$$g^{\text{lc}}_{F_d,E}(t_{\text{adj}}) = g^{\text{f}}_{F_d,E}(t_{\text{lc}}) + \Delta g_{F_d,E}(t_{\text{adj}}), \qquad (18)$$

where E_{lc} highlights the fact that $D_{E,\text{lc}}$ is used in the computations. The safe vehicle following distances to vehicles at the destination lane are computed using the time $t = t_{\text{lc}}$, because the gaps between them and E must be safe by the time the maneuver is completed. Once the lane change is done, E can revert back to using D_E in its computations. The total necessary gap at the destination lane is:

$$g_{\text{dest}}(t_{\text{adj}}) = g^{\text{lc}}_{E,L_d}(t_{\text{adj}}) + l_E + g^{\text{lc}}_{F_d,E}(t_{\text{adj}}). \qquad (19)$$

3.4.   Numerical Results

The proposed methods are evaluated in simulation with realistic values. Two vehicle types are used: passenger vehicle and trucks. Their parameters are detailed in table 1. It should be noted that some of these parameters depend on the current speed, but they are set constant to ease visualization and analysis.

Let's start by analyzing how safe vehicle following spacings vary with relative speed and different vehicle types. In Figure 4, each plot represents an ego vehicle/ leader combination: passenger vehicle/ passenger vehicle (PP), passenger vehicle/ truck (PT), truck/ passenger vehicle (TP), and truck/ truck (TT). The red lines represent the vehicle following gap from Eq. (10) and the color map indicates collision severity for the vehicle of lowest mass. In all cases, the leader's initial velocity is $v_L(t_0) = 90km/h$ and, when computing the time headway, the ego vehicle assumes $\rho = 0.9$, and $\bar{v}_E = 108km/h$. Moreover, if both vehicles are of the same type, we assume the ego vehicle to brake at most with γD_{max}, where $\gamma = 0.85$. The computed vehicle following gap is an overestimation of the non-linear collision free boundary as long as all initial assumptions on maximum decelerations and velocities hold. For the three cases where the follower cannot brake as
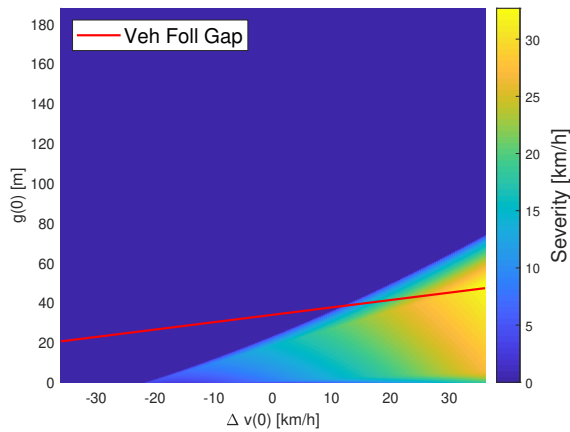
(a) Passenger vehicle following passenger vehicle.
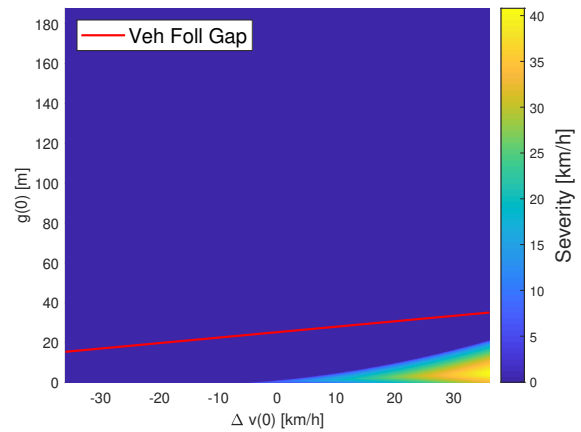
(b) Passenger vehicle following truck.
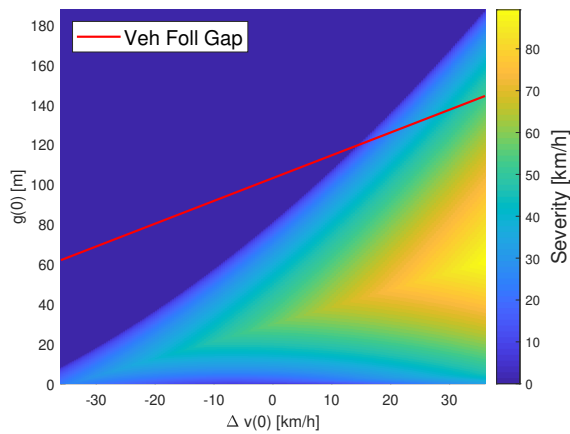
(c) Truck following passenger vehicle.
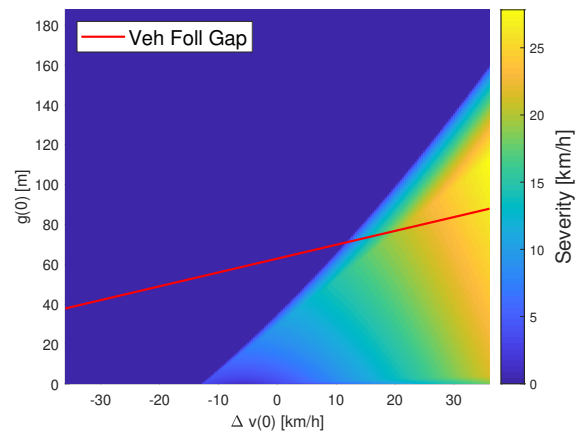
(d) Truck following truck.

Figure 4: The red line represents the minimum safe vehicle following distance as a function of the relative velocity The color map indicates the severity, as computed from Eq. (4), of a collision under the described worst-case scenario for each combination of initial gap and velocity.

Table 2: Parameters for Lane Change Spacing.

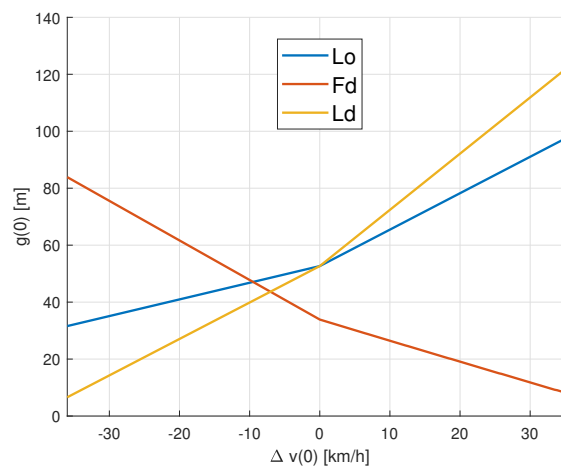| Parameter [unit]	Value
$H[m]$	3.6
$\Delta t_{\text{lc}}[s]$	5
$t_{\text{adj}}[s]$	0
γ_{F_d}	0.85
γ_{L_d} , γ_{L_o}	1.15
γ_E	1
$-D_{\text{LC}}[m/s^2]$	-4
$A_{\text{LC}}[m/s^2]$	0

Figure 5: Minimum lane change safe spacing from L_o (blue), F_d (red) and L_d (yellow) as a function of relative velocity.

hard as its leader (Figs. 4a, 4c and 4d), the gaps are conservative while $v_E(0) \leq \min[v_L(0)/\rho \, , \bar{v}_E]$. A well designed vehicle following controller can keep the vehicle within these limits. In the case when the follower has a greater braking capability than its leader, the assumption for the closed form solution of Eq. (5) is no longer respected and, thus, the computed safe gap is conservative for the whole relative velocity range. Comparing the four plots, it is clear that trucks need larger spaces ahead of them than passenger vehicles and that mass differences lead to different maximum severities.

Next, safe lane change spacings are computed. The scenario includes four passenger vehicles with maximum deceleration $D_k = \gamma_k D_{\text{max}}$, where $k = \{L_o, L_d, E, F_d\}$. The values of ρ and $\bar{v}$ are as in the previous experiment. Table 2 provides values for γ_k's along with the other required parameters. Figure 5 shows the minimum gaps to each vehicle as a function of relative speeds when all but the ego are traveling at $90km/h$. The results agree with intuition: the faster the ego vehicle is traveling, the farther away from its leaders in the original (L_o) and destination lane (L_d) it must be. The converse is true regarding its follower in the destination lane (F_d). Moreover, we
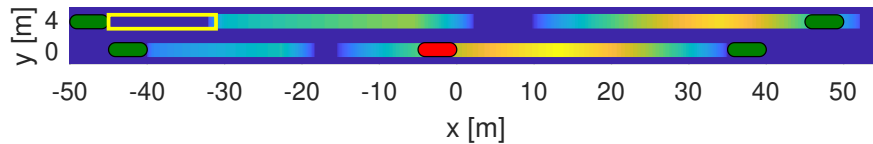
Figure 6: Risk map for the red ego vehicle. All vehicles are moving from left to right and the color map represents collision severity for the worst case scenario. On top, results considering only vehicle following. On the bottom, the risk map when lane change factors are taken into account. The yellow rectangle shows the expected relative distance variation during the maneuver.

see how safe distances increase more sharply once the ego vehicle is faster than its leaders. This effect is due to non-linearities in the transient lane change gap.

Last, these results can be used to create a risk map of the ego vehicle's surroundings. Let there be a scenario with parameters as before: followers have less and leaders have more braking capability then E. Moreover, vehicles in the origin lane are all traveling at $90 km/h$ and vehicles at the destination lane are all traveling at $100 km/h$. For comparison, a risk map that considers only safe vehicle following is shown at the top of Figure 6. It is clear that the red ego vehicle is at a safe position in its original lane if there is no intention for lane changes. The bottom of the same figure presents a risk map which explicitly takes lane change into account. The rectangle with yellow edges shows $\Delta g_{F_d,E}(t)$, the gap variation between F_d and E during a lane change. Therefore, the accident prone area in front of F_d is shifted forward to represent the situation at the end of a possible lane change. Another visible difference is the increase of the risk areas behind both leaders. This is a consequence of E's reduced maximum braking during lateral movement. This risk map helps to show how finding safe lane change spacings is challenging and why the communication between vehicles is necessary.

4   Lane Changing Protocols

In this section, we present the communication protocol to be followed by vehicles involved in the lane change. We define which parameters must be exchanged by vehicles, how the communication should occur to allow for gap generation requests and how to deal with conflicts.
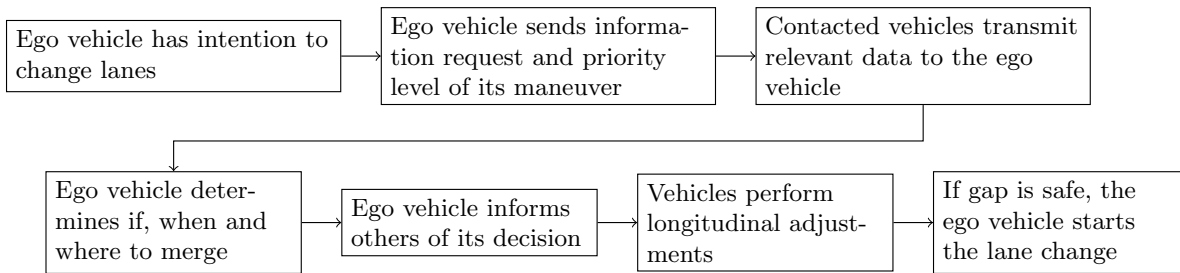
Ego vehicle has intention to change lanes	→	Ego vehicle sends information request and priority level of its maneuver	→	Contacted vehicles transmit relevant data to the ego vehicle

Ego vehicle determines if, when and where to merge	→	Ego vehicle informs others of its decision	→	Vehicles perform longitudinal adjustments	→	If gap is safe, the ego vehicle starts the lane change

Figure 7: Communication protocol for lane change.

4.1.   Communications

Safety applications built to operate on connected scenarios commonly use Basic Safety Message (BSM) packets, which are sent at a 10 Hz frequency and whose typical communication range is around $500m$ [27, 41]. These packets contain data such as vehicle size, position, speed, and acceleration. To compute the lane change safe gaps, E requests, in addition: mass, width, and maximum acceleration, deceleration and jerk of its surrounding vehicles. Furthermore, if the gap on the destination lane is too small, E can request F_d to lower its speed and create a big enough space. This procedure has two benefits. First, it improves maneuver safety, since no one has to force itself on a risky position at the destination lane. Second, it prevents vehicles from being stuck on a lane. This is particularly detrimental for vehicles trying to move towards a highway exit or trying to leave a merging lane. Moreover, having such a procedure is fundamental for platoons, since they demand more space to merge as is shown further on.

The communications to set up the maneuver must follow some predefined protocol. An overview of our proposed method is presented in Fig. 7. The details for each step are:

Ego vehicle has intention to change lanes: it is assumed that a higher level algorithm determines not only whether the vehicle wants to change lanes, but also why. The reason to perform a maneuver is used further on for conflict resolution, i.e., when several vehicles are trying to change lanes in the same region.

Ego vehicle sends information request and priority level of its maneuver: the ego vehicle has to modify its next message sent through DSRC to include a request for more information about those within its range. In addition, E also informs others about its maneuver priority, which depends directly on the reason for the intention to change lanes. The different priorities are described later on together with the conflict resolution rules.

Contacted vehicles transmit relevant data to the ego vehicle: each vehicle sends two sets of data to E. The first one contains the vehicle's own parameters: length, mass, width, and maximum acceleration, deceleration and jerk, as well as their current speed and acceleration. The second set informs whether the contacted vehicle is willing to cooperate with the maneuver and whether there is a conflict.

Ego vehicle determines if, when and where to merge: having all the necessary data, the ego vehicle checks whether it can merge under the current traffic state. If necessary, it might wait for

other maneuvers to end. In low density situations, the ego vehicle can opt to perform lane change
with non-zero relative speed to vehicles in the adjacent lane, and to adjust its velocity afterwards.
However, under congested scenarios, the current gaps are not large enough and E has to choose
which vehicle will generate the proper spacing.

Ego vehicle informs others of its decision: E uses the vehicles' unique identifiers to specify
which one should become its follower on the destination lane and it shares its own parameters with
this vehicle. This allows F_d to know the size of the gap to generate for E. Moreover, all vehicles
within range are aware that a lane change is taking place and can monitor for conflicts.

Vehicles perform longitudinal adjustments: F_d adjusts its distance to L_d until the gap is big
enough for the ego vehicle to merge. At the same time, E must ensure it does not overtake L_d,
while keeping a safe distance to L_o. The controller that achieves these objectives is presented
further on in this report.

If gap is safe, the ego vehicle starts the lane change: the ego vehicle continuously monitors the
three relevant spacings with its onboard sensors and starts the maneuver when they meet the safety
requirements.

4.2.   Conflict Resolution

When the ego vehicle starts communicating with others, it informs its lane change priority level
as:

1. Urgent: lane change to avoid high risk situation;

2. High: mandatory lane change, such as merging;

3. Medium: lane change towards a route goal, such as reaching an exit;

4. Low: discretionary lane change to achieve higher speed.

To deal with possible conflicts, any vehicle which receives a request keeps the priority information
stored until the maneuver is finished or up to a certain expiration time limit. If this vehicle receives
another request, it identifies a possible conflict. If two requests have the same priority, they are
treated in a first come, first served basis. If a higher priority request arrives to a certain vehicle, it is
this vehicle's responsibility to determine whether the maneuver requested earlier should be delayed
and then perform the proper communication. Since each lane changing vehicle may communicate
to several others in the adjacent lane, we can define a minimum number of vehicles between two
possible new gaps. In other words, if the lane changes are longitudinally far from each other, they
may happen simultaneously.

5   Lane Changing and Merging of Platoons

This section extends previous results of single-vehicle lane change to vehicle platoons. A platoon is
a group of vehicles with similar characteristics that use communication to follow each other closely

and safely. Platoons are shown to improve road utilization in works such as [3]. Moreover, truck platoons are motivated both from the lack of truck drivers and from drag reduction which improves fuel economy. The study of platoon lane changes is therefore important to avoid the situation where each vehicle negotiates its maneuver independently. The free-for-all approach has at least two clear disadvantages when compared to a unified platoon strategy. First, in the former, there would be several vehicles on the original lane trying to communicate to vehicles at the destination lane at the same time, while, in the latter, a single platoon vehicle can establish communication and negotiate for the whole platoon. Second, if each one does their maneuver individually, there will no longer be a platoon after the lane change. In what follows, we first determine the total space which has to be generated at the destination lane for a platoon to safely fit. This step helps to quantify the disturbance created in the destination lane. Then, we present three platoon lane changing strategies which describe how the platoon vehicles can use the gap being generated for them.

5.1.   Spacing for Platoon Lane Change

Let's start by analyzing some of the platoon's characteristics. When it is at steady-state:

$$
\begin{aligned}
v_n(t) =& v_P(t) && \forall n, \\
g_{n,n-1}(t) =& h_n v_P(t) + d_{0,n}, && \forall n,
\end{aligned}
\tag{20}
$$

where v_n is the speed of vehicle p_n and v_P is the platoon speed. The index $n \in [1, N]$ represents the vehicle's position in the platoon, with 1 being the platoon leader and N being the last vehicle. These assumptions yield a platoon length of

$$
l_P(N, t) = l_1 + \sum_{n=2}^{N} (h_n v_P(t) + d_{0,n} + l_n),
\tag{21}
$$

where l_n is the vehicle's length. If vehicles are uniform, we define $l_n = l$, $h_n = h$ and $d_{0,n} = d_0$, $\forall n$, and the above formula is simplified to:

$$
l_P(N, t) = Nl + (N-1)(h v_P(t) + d_0).
\tag{22}
$$

We note that the platoon length grows as a function of the number of vehicles N, the traveling velocity $v_P(t)$, and vehicles' characteristics l, h and d_0. Extending the single vehicle result to platoons, the necessary gap at the adjacent lane is:

$$
g_{\text{dest}}(t_{\text{adj}}) = g_{p_1, L_d}^{\text{lc}}(t_{\text{adj}}) + l_{P,\text{lc}}(N, t_{\text{adj}}) + g_{F_d, p_N}^{\text{lc}}(t_{\text{adj}}),
\tag{23}
$$

where $l_{P,\text{lc}}(N, t_{\text{adj}})$ is the length of the platoon after vehicles update their braking capabilities from D_p to $D_{p,\text{lc}}$. By construction, $l_{P,\text{lc}}(N, t_{\text{adj}}) > l_P(N, t_{\text{adj}})$, which means that platoon vehicles must increase their distances to each other before starting the maneuver. After completing the maneuver, they can go back to the original inter-vehicle gaps. The first and last terms of the necessary gap
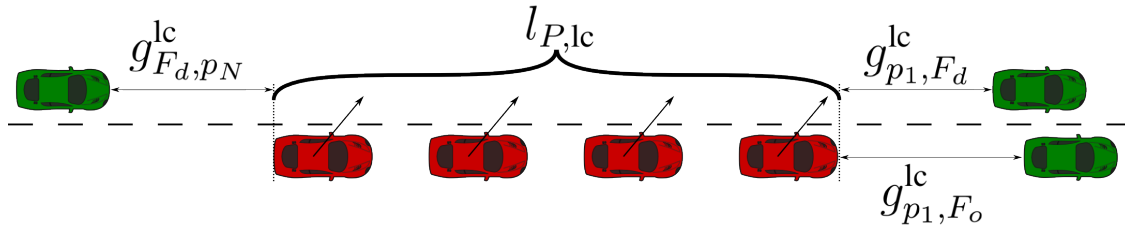
Figure 8: The platoon of red vehicles waits for a proper spacing on the adjacent lane before they can start a synchronized maneuver.

are similar to the single vehicle case, with E being substituted by p_1 and p_N respectively. Thus, the platoon length quantifies how much more disturbance is caused in the destination lane due to a joint platoon maneuver.

5.2. Lane Changing Strategies

The platoon vehicles can use the gap being created at the destination lane in different ways. In unexpected cases, such as L_d or L_o performing emergency braking after the platoon has started changing lanes, the joint maneuver is aborted and the platoon is split in two: one formed by vehicles already in the destination lane and one by vehicles still in the origin lane.

5.2.1. Synchronous

The first strategy is to have the all platoon vehicles performing the maneuver simultaneously. This requires that gaps from p_1 to L_o and L_d and from F_d to p_N respect the safety conditions:

$$g_{i,j}(t) \geq g_{i,j}^{\text{lc}}(t), \tag{24}$$

where the pairs $(i, j) = \{(p_1, L_o), (p_1, L_d), (F_d, p_N)\}$ and the safe lane change gaps follow from Eqs. (16) to (18) respectively. Regarding communications, the platoon leader p_1 is responsible for exchanging messages with vehicles in the destination lane. Figure 8 illustrates this strategy and the minimum spacings. The main drawback of this approach becomes visible: the wait for such a big gap leads to road sub-utilization.

5.2.2. Leader First

Instead of waiting for a spacing that fits the entire platoon, vehicles can move in one at a time while the gap in the adjacent lane is being generated. Therefore, each platoon vehicle only has to observe safe conditions for itself before starting the maneuver. The platoon leader is again responsible for communications. It monitors distances to the same three vehicles as before: L_o, L_d and F_d, as illustrated by Figure 9. For p_2, determining who is the leader on the current lane and on the destination lane depends on the time p_1 takes to move in the other lane. If $g_{F_d,p_2}(t) \geq g_{F_d,p_2}^{\text{lc}}(t)$
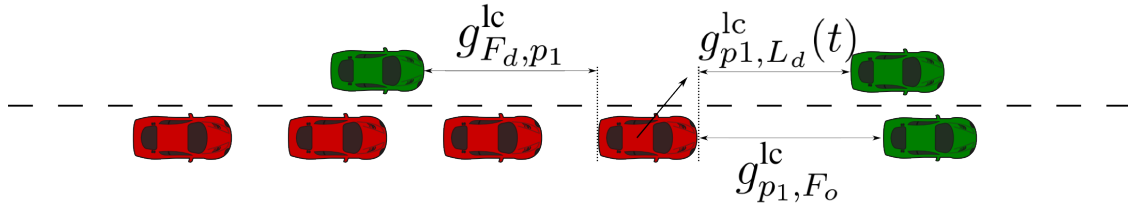
Figure 9: As soon as the platoon leader observes the gaps are safe, it can start lane changing.
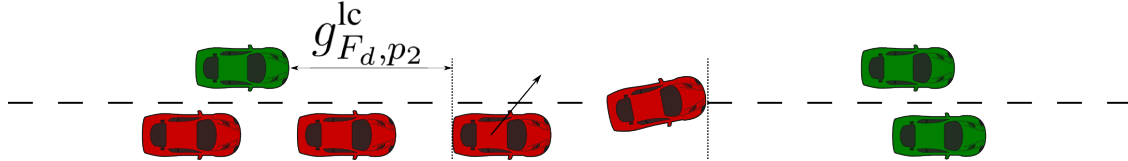

Figure 10: If the distance from F_d to p_2 is safe and p_2 doesn't even "see" L_o yet, p_2 can start lane changing.

is satisfied before p_1 finishes its maneuver, p_2 only has to keep track of two distances, as in Fig. 10. The other possibility is that p_1 finishes the lane change while p_2 is still waiting. Under normal operation, after p_1 changes lanes, $g_{p_2,L_o}(t) > g^{\text{lc}}_{p_2,L_o}(t)$, but p_2 must keep track of L_o anyway to avoid collisions in case L_o has to brake. The relevant gaps are shown in Fig. 11. This reasoning is easily extended for $2 < n \leq N$.

The main advantage of this strategy is that, while the platoon waits for the gap to be generated, there is no longer a growing empty region on the road. This improves road utilization. The lane changing vehicles still need to increase the distances to their respective leaders before initiating any lateral movement and to reduce it after finishing the maneuver.

5.2.3.   Last Vehicle First

In the "Last Vehicle First" strategy, the last platoon vehicle, p_N, is the first to change lanes. Afterwards, it creates the proper spacing for the others. Therefore, it is now p_N who communicates with vehicles in the adjacent lane and it monitors gaps to p_{N-1}, L_d and F_d to determine when it is safe to start lane changing. Fig. 12 depicts this approach. Concerning the rest of the platoon, vehicle n, $n \in \{2, N-1\}$, keeps track of the distances to $n+1$, L_d and $n-1$, which became its follower on the destination lane. Lastly, p_1 monitors L_o, L_d and p_2.

The advantage of this behavior over the previous strategy is that F_d only has to actively create space for one vehicle and then it can go back to regular vehicle following behavior. One drawback shows up when the whole platoon must merge into the adjacent lane before a certain point upstream. In this case, the platoon leader, which is the first vehicle to reach the merging point, should also be the first to change lanes.
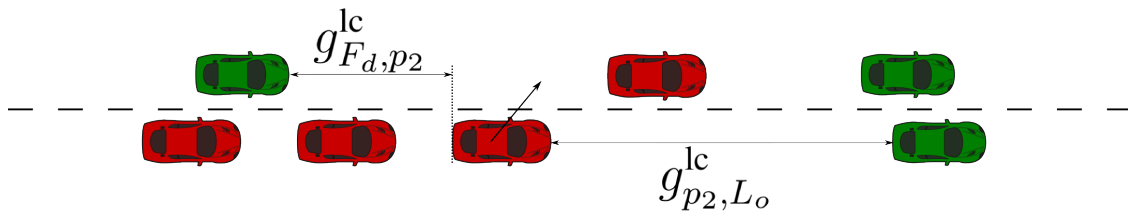
Figure 11: Vehicle p_2 has to check its distance to L_o to be able to react in case something unexpected happens.
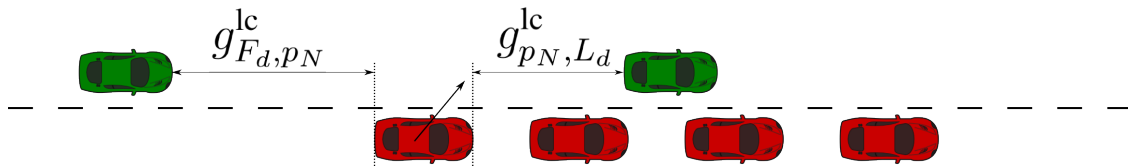

Figure 12: Vehicle p_N negotiated the maneuver and starts its lateral movement as soon as gaps are safe.

5.3.   Numerical Results

As in the experiments of section 3, two vehicle types are used in simulations: passenger vehicles and trucks. Their parameters are detailed in table 1. The safe gaps from p_1 to L_o and L_d and from F_d to p_N are the same as in the single vehicle case. The interest now is how $g_{\text{dest}}(F_d, L_d)$ varies with the platoon's velocity, size and type. The parameters H, Δt_{lc}, t_{adj} and the passenger vehicle's maximum deceleration during lane change are all as in table 2. In addition, a truck's maximum braking during lane change is set to $-2m/s^2$.

Let's first analyze how relative velocities and the number of vehicles in the platoon affect the necessary gap at the adjacent lane. For that, let all vehicles be passenger vehicles and all but the platoon vehicles be traveling at a speed of $90km/h$. Fig. 13 shows the necessary gaps as a function of relative velocity between lanes for different platoon sizes. Inter-platoon gaps, which influence platoon length, increase quickly with speed because the time headway when preparing for a lane change is larger than the regular vehicle following headway. Therefore performing the maneuver at lower velocity decreases the spacing requirement considerably. However, this also requires a large gap from F_d to p_N (as in the previous result of Fig. 1) which is not common in congested scenarios.

To see how the spacing requirements change when trucks are involved, a truck platoon is simulated. The number of vehicles in the platoon is fixed at $N = 5$ and the surrounding vehicles are again traveling at $90km/h$. Fig. 14 shows the necessary gaps as a function of relative velocities between lanes for two situations. In blue, the platoon is merging between other two trucks, while, in red, it is merging between two passenger vehicles. Clearly the truck platoons demand much bigger spaces to safely lane change.
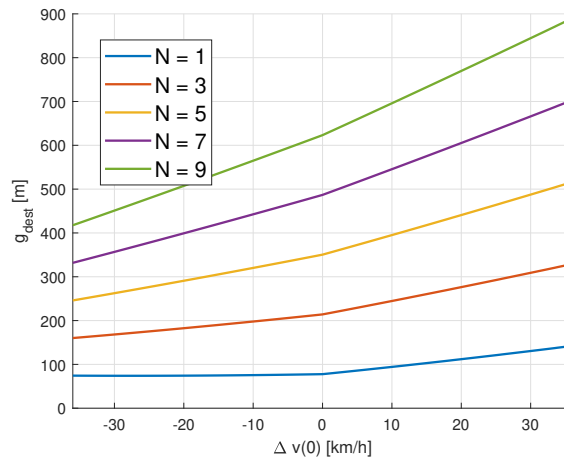
Figure 13: Minimum gap at the adjacent lane as a function of the relative velocity between lanes for different number of vehicles in the platoon.
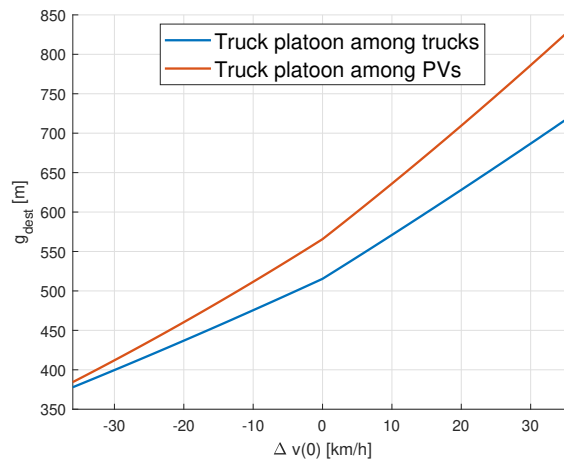

Figure 14: Minimum gap at the adjacent lane for a five vehicle truck platoon as a function of the relative velocity between lanes. In blue, the truck platoon merges between trucks and, in red, it merges between passenger vehicles.

6 Validation and Verification of Safety Spacing

This section presents methods and requirements to guarantee that a vehicle can safely determine whether the necessary gaps for lane change have been created. This includes an analysis of the information sources available, a protocol to verify whether measurements are reliable and techniques to identify and assess possible failures.

6.1. Information Sources

Once the gap generation procedure starts, the ego-vehicle E must monitor its distances and relative velocities to the three relevant surrounding vehicles: the leader at the origin lane (L_o), the follower at the destination lane (F_d) and the leader at the destination lane (L_d). Lane changing can only start after the safe gaps developed in section 3 are respected. Fig. 15 illustrates the situation and the ego vehicle's sources of information to verify that safety conditions are met. These sources are:

- Sensors: the ego vehicle is assumed to have at least N independent sensors to measure the gap and speed of each of its relevant surrounding vehicles. Example: radar, LiDAR, camera.

- Communications: other vehicles provide some of their parameters, such as mass and maximum deceleration once, and then periodically send E their position, velocity, and acceleration. V2V safety applications are commonly built around Basic Safety Message (BSM) packets, which are sent at a 10 Hz frequency and whose typical communication range is around $500m$ [27]. These values fulfill our requirements. Example: DSRC, 5G.

- Dynamical Model: E has a model of its surrounding vehicles and uses it to estimate the value of the next measurement coming from sensors or communication. Example: double integrator with input disturbance.

6.2. Verification Protocol

A flowchart of the failure verification procedure for each surrounding vehicle is shown in Fig. 16. This procedure happens in a loop at every Δt seconds. The interval length value is defined based on safety standards and computational capacity. All sensors measure the gap and the relative velocity between the ego and the other vehicle. Moreover, through communications, the other vehicle informs its current GPS position, velocity, and acceleration. The first two values allow E to obtain another measurement for the gap and the relative speed. In addition, E's internal dynamical model of the other vehicle uses the acceleration and velocity acquired through communications to make predictions of the gap and the relative speed. The dashed arrow from Communications to Dynamical Model indicates that the latter uses data provided by the former. All these data sources report their values to a consistency check system. If no inconsistencies are found, the maneuver goes on. Otherwise, a failure identification procedure starts. Once the failure is identified, another system assesses the failure severity. Based on this evaluation, the vehicle can either proceed with the maneuver or abort it and warn the driver.
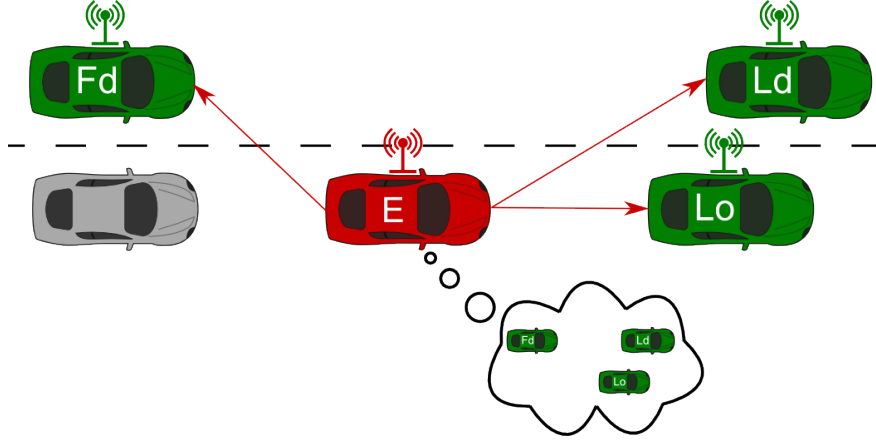
Figure 15: The ego vehicle monitors its surrounding vehicles. Arrows indicate sensor measurements, an antenna indicates the vehicle is communicating, and the thought bubble represents E's internal model of the others.

6.3.   Consistency Check and Failure Identification

The protocol described above runs periodically at every Δt seconds. At each computation cycle k, where $k \in \mathbb{N}$, we use the sensors' and communications' most recent data. The dynamical model, on the other hand, can provide state estimates at any desired time instant. Given the vehicles' accelerations at some time $t' < k\Delta t$, the model computes expected values for relative velocity and gap at $k\Delta t$.

To characterize how the consistency check works, let $x_i(k)$ be the most recent measured/ estimated value of variable x by source i at the beginning of computation cycle k. The possible data origins are $i \in \{s_1, s_2, \ldots, s_N, c, m\}$, where s_n, c and m indicate the information came from sensor n, communications or model respectively. All measurements are compared with each other and checked against a threshold. We can express the pairwise comparison results as:

$$r_{ij}(k) = \begin{cases} 0, & \text{if } |x_i(k) - x_j(k)| \leq \epsilon_{ij} \\ 1, & \text{otherwise.} \end{cases}, \ \forall j \neq i. \tag{25}$$

where ϵ_{ij} is a threshold which depends on factors such as sensor noise, communications delay and model accuracy. If $r_{ij}(k) = 0, \forall i, j$, there are no inconsistencies and the maneuver can proceed as planned. Otherwise, an inconsistency is detected and the failure identification process is activated. A failure mode i is identified if source i disagrees with half or more of the others. Mathematically:

$$\sum_{j \neq i} r_{ij}(k) \geq \frac{N+1}{2} \implies \text{failure mode } i \text{ at cycle } k, \tag{26}$$

where $N + 2$ is the total number of sources. Given that sensors are independent and with a short enough Δt, we can assume at most one new failure occurs per cycle.
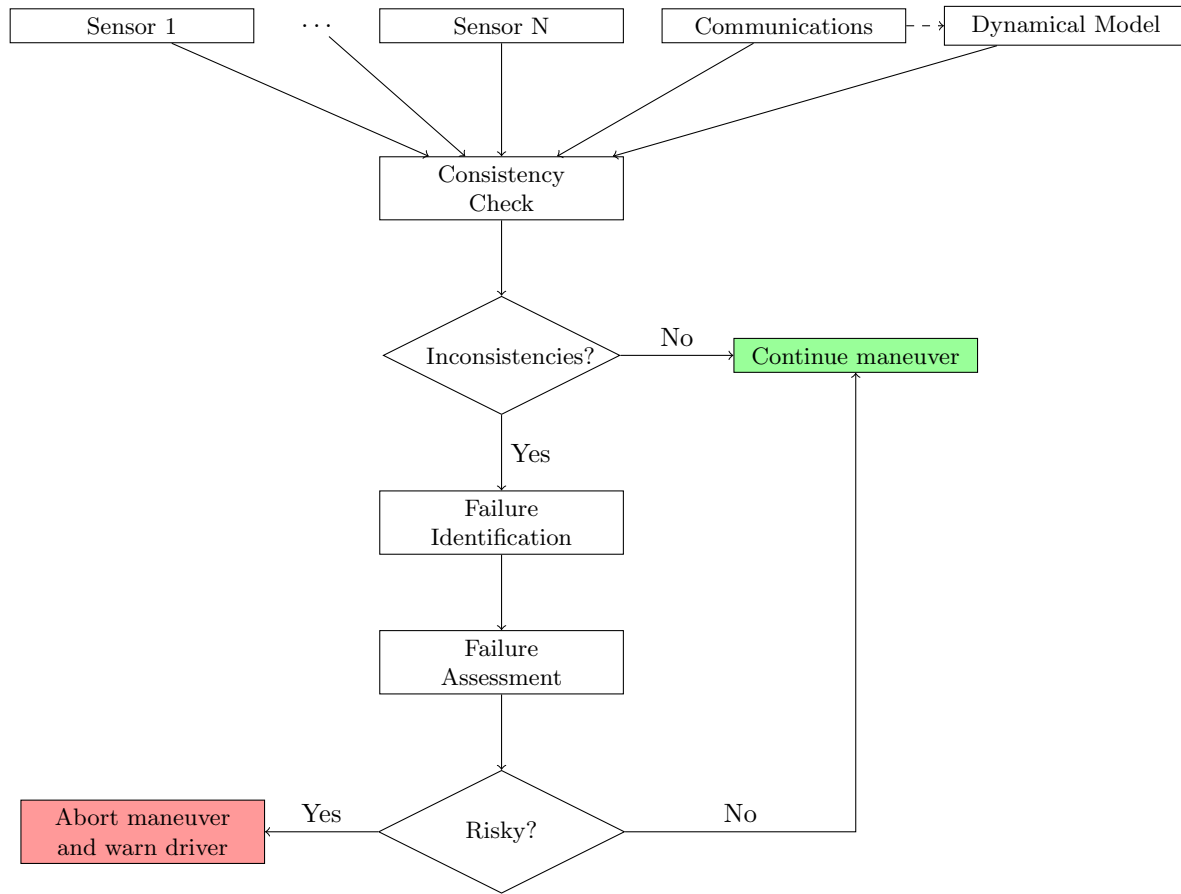
Figure 16: Flowchart of verification procedure with N independent sensors.

6.4.   Failure Assessment

Not all failure modes have the same effect on the ego vehicle's ability to verify the gap. Let's study the impact of each one.

6.4.1.   Sensor Failure Mode

Once a sensor failure is identified, the driver gets a non-emergency warning and that sensor's measurements will be ignored until it is fixed. This failure is considered not risky. To guarantee some redundancy, and therefore safety, we require at least two working sensors at all times. Thus, if a second sensor failure is identified further on, the risk is considered high enough so that the maneuver is aborted and the driver is requested to take control of the vehicle. We define f_{s_n} as the failure mode of sensor n and the failure mode for less than two working sensors is called F_s.
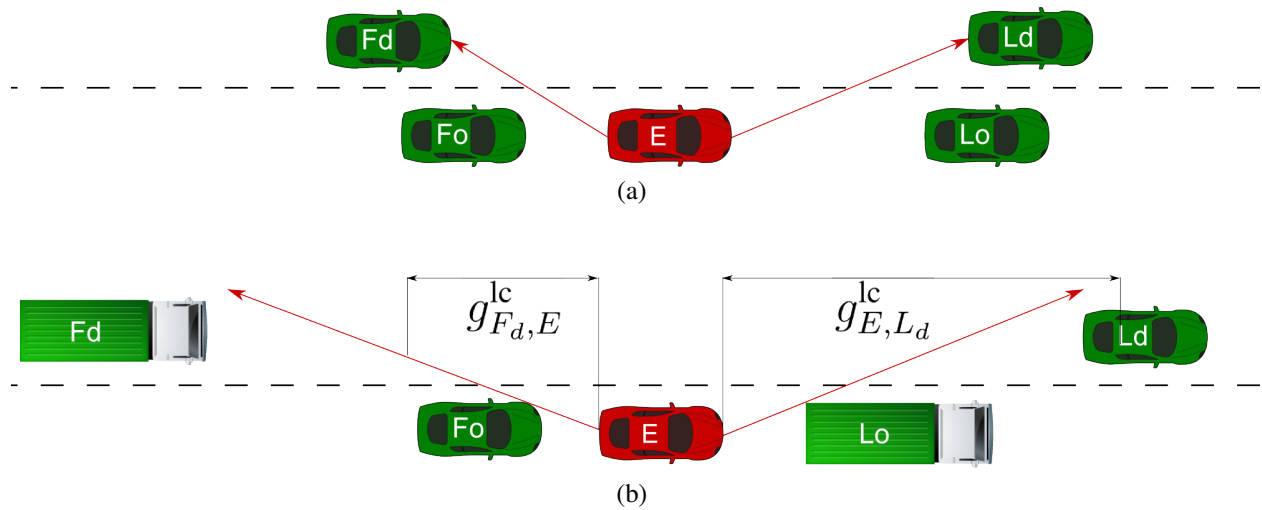
Figure 17: Ego vehicle visibility of vehicles on the destination. On top, all vehicle are visible. At the bottom, a configuration where follower and leader on the origin lane "hide" their counterparts at the destination lane. Red arrows indicate E's measurements and black arrows show the safe lane change gaps.

6.4.2. Communication Failure Modes

We assume the ego vehicle is already communicating periodically with all the surrounding vehicles when a failure is detected. We do this because, if issues in communication arise before the initial contact phase (or if communication is not even established), the gap generation procedure wouldn't have started at all. When the failure mode in communication f_c is identified, the ego vehicle will increase its desired safe distance to the other vehicle to account for the loss of reliable information. Moreover, the dynamical model will use the last trustworthy data from the communications system to compute its next estimate. This affects the failure detection thresholds of the consistency check block. Furthermore, if the communication failure is persistent after K cycles, the dynamical model starts using data provided by the sensors.

To evaluate the severity of failure mode f_c, it is necessary to check whether the other vehicle's states can be measured by the ego vehicle's sensors. While the leader in the origin lane, L_o, is always visible to E, follower and leader in the destination lane, F_d and L_d respectively, might be shadowed by vehicles in the origin lane. Fig. 17 shows, on top, a situation where both are visible. A configuration where vehicles at the origin lane prevent E's sensors from obtaining measurements of the vehicles on the destination lane is depicted at the bottom.

The scenario in which L_o conceals L_d is more likely to happen either when $v_{L_o} < v_{L_d}$ or when L_d has higher braking capability than L_o, which forces E to keep a bigger gap to its virtual leader than to its real leader. A similar analysis holds true for the case of F_o concealing F_d. In both cases, we have to analyze not only if the vehicle in the destination lane is visible, but also whether the visibility range includes the safe lane change gap. In the illustration at the bottom of Fig. 17, the ego vehicle cannot check whether the safe gap to L_d is respected, but it can ascertain that F_d is far
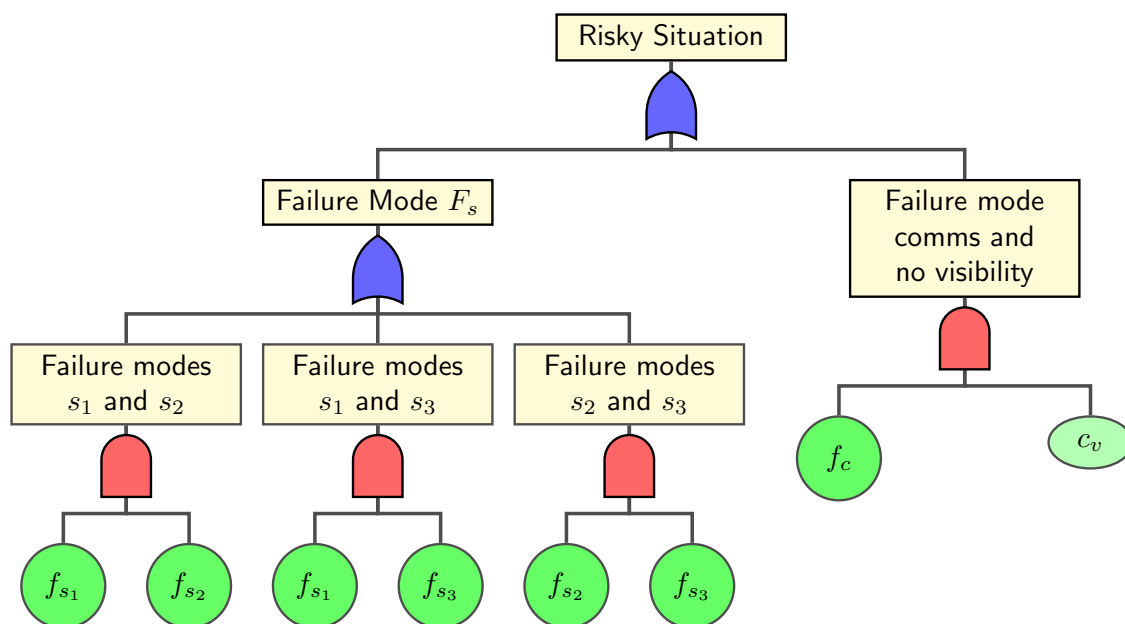
Figure 18: Fault Tree for gap verification

away enough. Following this reasoning, we define a conditioning event c_v which indicates that E cannot verify the safe gap with it's sensors. Then, failure mode f_c is assessed as not risky if the ego vehicle's field of view includes the other vehicle or the safe gap. Otherwise, the system identifies a risky situation and proceeds accordingly.

6.4.3.   Risk Assessment Tree

Assuming three sensors, Fig. 18 summarizes the behaviors described above. The basic event f_i represents failure mode $i \in \{s_1, s_2, s_3, c\}$ and c_v is the conditioning event where E's sensors cannot check if the safe gap is respected.

7   Minimize Impact on Traffic Flow

In this section, we present control strategies that minimize the lane change impact on traffic flow while guaranteeing strict safety constraints. We start by characterizing the several phases of the maneuver, which include longitudinal adjustments before and after the lane change per se. Then, we present the longitudinal control policy that is responsible for: creating safe gaps in the destination lane, increasing gaps to account for loss in braking capability during lateral movement and keeping the lane changing vehicles in the proper longitudinal position. The proposed method is shown to have two important characteristics that minimize impact on traffic. First, whenever a vehicle must increase the distance to its leader, the controller ensures asymptotic convergence to the new gap and velocity setpoint. Secondly, it guarantees string-stability. Simply put, string-stability means that disturbances are attenuated by following vehicles (for a more formal definition

the reader is directed to works such as [40]). Without this characteristic, vehicles upstream would slow down more than vehicles involved in the maneuver, negatively impacting traffic flow and possibly creating stop-and-go behavior. The section ends with the presentation of the lateral controller, responsible for taking the vehicle from one lane to the other once the gaps are safe. This controller also presents asymptotic convergence and is based solely on measurements obtained by the vehicle's sensors.

   The techniques presented in this section provide analytical guarantees for the desired behaviors. Impact minimization decisions that rely on simulation results, namely which platoon strategy is best for each scenario, are discussed in section 8.

7.1.   Lane Change Phases

When analyzing the lane change impact on traffic, we want to look at the whole process including the adjustments before and after the lane change has taken place. This is particularly important because of our interest in congested scenarios, where there is initially no available safe gap to merge. The different phases of the maneuver are:

0. Vehicle following: $t \leq t_0$
   The situation preceding any adjustment towards the lane change is depicted in Fig. 19a. Before t_0 vehicles perform lane keeping and autonomous vehicle following. By $t = t_0$, the ego vehicle E, in red, has already performed the necessary communications. Its follower F_d and leader L_d at the destination lane have been determined and the longitudinal adjustments may start. This phase serves to describe the initial state of the system and is not considered when computing maneuver impacts.

1. Longitudinal adjustments: $t_0 < t \leq t_{\mathrm{adj}}$
   During this phase both lanes are affected by vehicles' longitudinal adjustments. If there is no safe spacing into which E can move, F_d starts decelerating to create a big enough gap. By the end of F_d's adjustment it should be at a safe vehicle following distance, $g_{F_d,E}(t_{\mathrm{adj}}) \geq g_{F_d,E}^{\mathrm{lc}}(t_{\mathrm{adj}})$. Concurrently, E also decelerates to create safe lane changing gaps to its leaders in the original and destination lanes. It is important to remember that gaps for safe lane changing are always larger than gaps for safe vehicle following since the former assumes a decreased braking capability of the ego vehicle. The time t_{adj} is determined by whichever vehicle, E or F_d, takes longer to achieve the new desired relative positions. Fig. 19b describes the spacings at this moment.

2. Lateral movement: $t_{\mathrm{adj}} < t \leq t_{\mathrm{lc}}$
   This is when the actual lane change occurs. Once all the gaps are safe, the ego vehicle can start turning its front wheels to create lateral movement. By $t = t_{\mathrm{lc}}$, the configuration is as in Fig. 19c. After the lane change, minimum safe following distances are respected.

3. Gap closing: $t_{\mathrm{lc}} < t \leq t_{\mathrm{f}}$
   After completing the lane change, vehicle E is farther away from its new leader L_d than
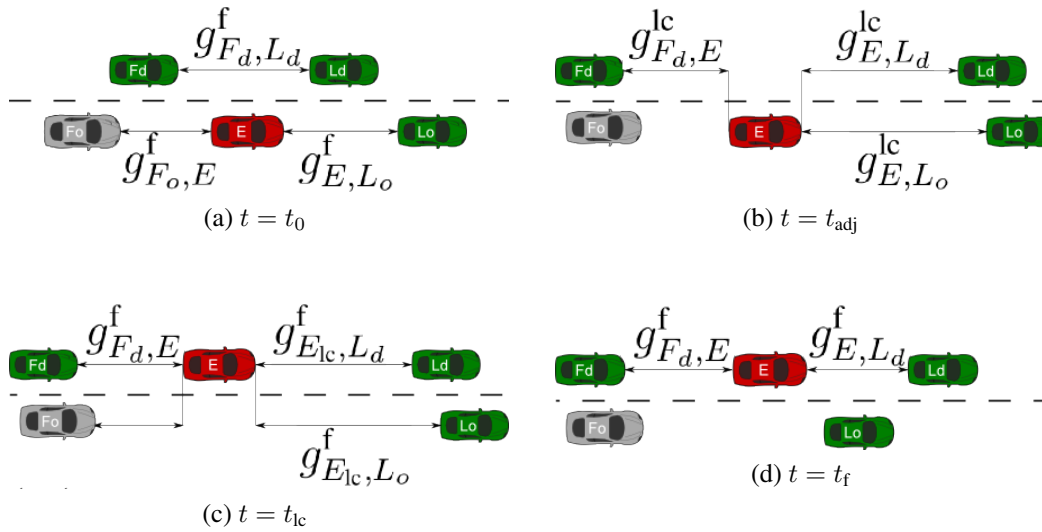
Figure 19: Examples of vehicle configurations at the different lane change phases. The red ego-vehicle must monitor the gaps to the three green vehicles F_d, L_d and L_o. The dependence of safe gaps on time is omitted to improve figure clarity.

needed for safe vehicle following. We recall that this is due to the fact that the ego vehicle takes its decreased braking capability into account when computing the lane change gaps. If at the beginning of the maneuver $v_E(t_0) \geq v_{L_d}(t_0)$, the gap by the end of the lateral movement phase is $g^{\text{lc}}_{E,L_d}(t_{\text{adj}})$. In this case, E will adjust its position to achieve the minimum safe following gap again, as shown in Fig. 19d. When this happens, at $t = t_{\text{f}}$, the maneuver is completed. Alternatively, if $v_E(t_0) < v_{L_d}(t_0)$, by the end of the lateral movement phase, L_d might be far away from E. In this configuration, we consider the maneuver completed at t_{f} such that $v_E(t_{\text{f}}) = v_{L_d}(t_{\text{f}})$.

Platoons of vehicles go through the same phases. The main difference is that, depending on the chosen platoon lane changing strategy, different vehicles might be at different phases at the same time instant. We define the platoon's initial and final maneuver times as $t_0 = \min_n[t_{0,n}]$ and $t_f = \max_n[t_{f,n}]$ where the $t_{0,n}$ and $t_{f,n}$ are the initial and final maneuver times for each platoon vehicle n. Let's analyze the phases at each of the strategies:

- Synchronous
  The only difference to a single vehicle maneuver is that, not only p_1 must increase its distance to L_o but also each platoon vehicle p_n, $n > 1$, must increase the distance to its respective leader p_{n-1} during the longitudinal adjustments phase. All vehicles start and finish the lateral movement phase together and then proceed to close the gaps to their respective leaders.

- Leader First
  In this case, while a vehicle is still on phase zero, another might have already finished its lateral movement phase. It is important to note that the gap closing phase only starts after all platoon vehicles have finished their lateral movement phase. This implies that, after

Figure 20: In (a), the left lane is moving faster than the right lane. The ego vehicle decided between which vehicles to merge and they can start creating the gap. Afterwards, in (b), F_d created the gap between itself and L_d, but, due to the relative speed between lanes, the gap is not at a suitable location for E.

completing their lane change, some vehicles keep constant speed waiting for the rest to finish their own lane changes.

- Last Vehicle First
  The analysis is similar to that of the Leader First case but the order in which vehicles enter each phase is reversed.

7.2. Gap Generation Controllers

We developed a cooperative decentralized control algorithm that enables the efficient creation of safe lane change gaps in congested scenarios while keeping strict collision avoidance constraints. The approach has the following characteristics: it guarantees that gaps are not only created, but also that they remain available where they are needed, it is easily adapted to different existing vehicle following policies and it requires little more tuning than the vehicle following controller itself. Moreover, it can be directly applied to platoons of vehicles, allowing them to keep their formation after the maneuver is complete.

To achieve that, we studied the most constrained steady-state scenario, where both lanes are at maximum capacity. This implies that all vehicles in the same lane travel at the same speed and the inter vehicle distances are minimum. A solution for this situation can be applied to any less constrained one.

Let's start by noting that, in the analyzed scenario, only F_d can generate the proper gap. The difficulty in this phase is one of synchronization: the gap between F_d and L_d needs to be big enough at a time when E is longitudinally between F_d and L_d. Therefore, merging with non-zero relative speeds would require precise control of several vehicles, which is an unrealistic demand for real-world cases. To see an example of this issue, let $v_{F_d}(t_0) > v_E(t_0)$ and let's have a moving reference frame fixed on E as in Fig. 20. The gaps on the adjacent lane are moving past E with a positive speed $v_{F_d}(t_0) - v_E(t_0)$ and E cannot accelerate to "catch-up" since its already following L_o at minimum distance. Thus, the gap would have to be created $[v_{F_d}(t_0) - v_E(t_0)]t_g$ meters upstream of E, where t_g is the time to generate the gap, and E would have to start its lateral motion precisely when the proper gap is passing by it. Even though we could try to guarantee safety by increasing the minimum gap, which would now also depend on the estimate of t_g and communication delays, the main drawback of allowing non-zero relative speeds would still exist:
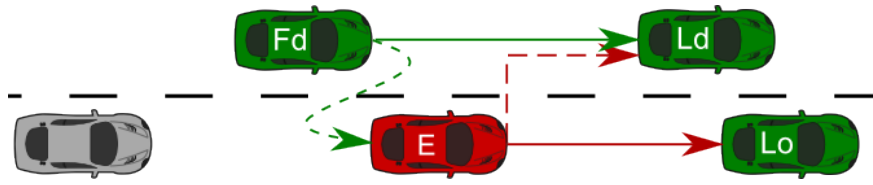
Figure 21: The solid arrows indicate the real leaders and the dashed ones indicates the virtual
leaders.

the risk of the gap "overtaking" E. In what follows, we initially provide a controller-agnostic
overview of the solution, that is, we describe the method in general lines so that it is not tied to a
specific vehicle following control law. Afterwards, the details for the chosen controller are shown
as well as the necessary changes to apply this approach to platoons of vehicles.

7.2.1. Approach Overview

To avoid the necessity of the previously described fine synchronization, we require that,

$$v_{F_d}(t) = v_E(t) = \min\left[v_{L_o}(t), v_{L_d}(t)\right].\tag{27}$$

by $t = t_{\text{adj}}$, the time when the lateral movement starts. To achieve this, we assign L_d as the virtual
leader of E and E as the virtual leader of F_d. A virtual leader is defined as vehicle which is
not in the same lane as the follower, but whose longitudinal position and velocity will be used
to determine the follower's acceleration. In Fig. 21 solid arrows indicates the real leaders and
the dashed ones indicates the virtual leaders. Under the above requirements, Eqs. (12) and (13)
show that the values of $\Delta g_{E,k}$, $\forall k$ will be zero or negative. Moreover, E can safely keep its speed
constant during the lane change, which yields:

$$g_{i,j}^{\text{lc}}(t) \le g_{i,j}^{\text{f}}(t),\tag{28}$$

where $(i,j) \in \{(E_{lc}, L_o), (E_{lc}, L_d), (F_d, E)\}$. Therefore, E (or F_d) has to observe simple safe
vehicle following distances to both L_o and L_d (or L_d and E).

In what follows, we focus our attention on how F_d behaves given both its real leader L_d and
its virtual leader E. During the longitudinal adjustments phase, $t_0 < t \le t_{\text{adj}}$, F_d computes two
control inputs in parallel. The one induced by the real leader is u_r and the one induced by the virtual
leader is u_v. The first is computed by whichever vehicle following law is responsible for keeping
a safe distance to L_d. The second input stems from the same control policy, but it is computed
based on errors to the virtual leader and it is not safety critical. To see why this distinction is
important, one can think of the case where, by t_0, the gap from F_d to E is close to zero, as in Fig.
21. Were the virtual following controller to react as sharply as the regular following controller, F_d
would brake as hard as possible. This would cause unnecessary great passenger discomfort at F_d.
Therefore, the virtual following controller should have parameters which yield smoother reactions,
such as lower maximum braking and jerk. Furthermore, if F_d is longitudinally ahead of its virtual

Table 3: Controller Differences

	Real Following	Virtual Following
Compute errors from:	real leader	virtual leader
Velocity control if:	leader far ahead	leader far behind
Outputs bounded by:	vehicle's dynamics	comfort constraints

leader, even a moderate deceleration might, with enough time, lead the vehicle to a very low speed. This behavior is again undesired given that the situation is not safety critical. Consequently, the virtual following controller should have a switching logic which keeps the vehicle at a constant minimum speed while F_d is still too far ahead of E. We note that a similar logic already exists in most regular vehicle following controller. They switch to free flow velocity control when the real leader is too far ahead or if there is no real leader. Table 3 summarizes the main differences between real and virtual vehicle following. Finally, to guarantee safety, after computing inputs from both controllers, F_d chooses the minimum - the hardest braking or the smallest acceleration - as its actual input. Thanks to this rule, we know that, at steady state, F_d will be at safe distance from E with close to zero relative speed.

One can apply the same reasoning to the ego vehicle following both L_o and L_d. Once E achieves steady-state, it will be at a safe vehicle following distance and at the same velocity of whichever leader is slower and at a larger than necessary distance to the other.

The proposed approach can be applied straightforwardly to most controllers which depend only on the vehicle's immediate preceding vehicle. This includes constant time headway controllers as well as some cited earlier such as [34] and [35]. However, making good use of communications, some laws also rely on the distance between a vehicle and the leader of its platoon [36, 40]. In these cases, vehicles can switch from their platoon leader dependent rule to one that relies only on their immediate leaders during the gap generation and lane changing processes.

7.2.2.   Chosen Vehicle Following Controller

Let the longitudinal dynamics of any vehicle k be modeled as a double integrator:

$$\begin{bmatrix} \dot{x}_k(t) \\ \dot{v}_k(t) \end{bmatrix} = \begin{bmatrix} 0 & 1 \\ 0 & 0 \end{bmatrix} \begin{bmatrix} x_k(t) \\ v_k(t) \end{bmatrix} + \begin{bmatrix} 0 \\ 1 \end{bmatrix} a_k(t), \tag{29}$$

and the acceleration be described by:

$$a_k(t) = u_k(t) + \Delta_{u_k}(t), \tag{30}$$

where u_k is the control input and Δ_{u_k} is a disturbance used to model non-linear effects. We opt for a constant time headway policy with headway and velocity errors defined respectively as:

$$e_h(t) = x_L(t) - l_L - x_E(t) - d_0 - hv(t), \tag{31}$$

$$e_v(t) = v_L(t) - v_E(t), \tag{32}$$

Pacific Southwest Region UTC
University Transportation Center

where the index L refers to either the real or virtual leader. It should be noted that the headway error is simply the current gap, as defined in Eq. (2), minus the desired gap from Eq. (10). Moreover, the value of the time headway h is chosen following Eq. (9), where parameter γ is obtained thanks to V2V communication. The control law for vehicle following is:

$$u_{foll}(t) = K_h e_h(t) + K_v e_v(t) + K_i \int_{t_0}^{t} e_h(\tau)\mathrm{d}\tau. \tag{33}$$

One desirable feature of vehicle following controllers is that they are string-stable. Assuming similar vehicles, it can be shown that:

$$h(hK_p + 2K_v) \geq 2 \tag{34}$$

is a necessary and sufficient condition for string-stability. Therefore, the controller gains can be determined by a slightly modified pole placement method that also guarantees string stability.

In case the leader is far ahead, it is assumed that there is no leader and the vehicle switches to a PI controller based on the error to the desired velocity. Similarly, in virtual following, if the virtual leader is too far behind, the controller switches to a PI which keeps the vehicle at its minimum accepted velocity. Moreover, two measures are put in place to produce a smooth behavior at setpoint changes. First, the desired gap goes through a low-pass filter to avoid abrupt control changes. Second, while E increases the distance to its real leader and as long as $g_{E,L_o}(t) \geq \alpha g_{E,L_o}^f(t)$, where $\alpha \geq 1$ is a design parameter, the maximum braking is limited to a comfortable value.

7.2.3.   Application to Platoons

When a platoon wants to change lanes, similar steps are taken. In the three strategies, F_d adopts p_N, the last platoon vehicle, as virtual leader and, consequently, creates a gap for the whole platoon. On the other hand, the definition of virtual leader for platoon vehicles depends on the strategy being employed. In the Synchronous case, only p_1 adds L_d as its virtual leader. Since the entire platoon changes lane simultaneously, vehicles p_n, $1 < n \leq N$ never have virtual leaders. When the Leader First strategy is used, p_1 follows the same procedure of a single vehicle. Then, as soon as any vehicle p_n, $\forall n$, finishes a lane change, p_{n+1} detects L_o as the new real leader and adopts p_n as virtual leader. Differently, the Last Vehicle First approach requires a change of virtual leader. When at the origin lane, p_n has p_{n-1} as real leader and L_d as virtual leader. During the time when p_n has completed the lane change phase, but p_{n-1} has not, p_n's real and virtual leaders are L_d and p_{n-1} respectively. In other words, p_n is p_{n-1}'s follower at the destination lane.

The other particularity of platoon lane changes arises when all platoon vehicles increase their gap setpoints to account for loss of braking capability during lateral movement. If all of them start their longitudinal adjustments simultaneously, an issue related to string-stability is verified. To see this, let the headway error of vehicle p_n be:

$$e_{h,n}(s) = G(s)e_{h,n-1}(s) + \zeta_n(s), \tag{35}$$

where $G(s)$ is the transfer function from headway error of preceding vehicle to headway error of following vehicle, and ζ_n models disturbances not caused by p_{n-1}. Without loss of generality, let $e_{h,n-1} = 0$. When vehicle p_n's setpoint changes, it has to increase its distance to p_{n-1}. This causes a disturbance

$$e_{h,n}(s) = \zeta_n(s) = F(s)\left[(h_{\text{lc}} - h)v_P + (d_{0,\text{lc}} - d_0)\right], \tag{36}$$

where $F(s)$ is a low-pass filter to create smooth changes, v_P is the platoon velocity, and h_{lc} and $d_{0,\text{lc}}$ are, respectively, headway and desired distance at standstill computed with lane change braking parameters. Next, note that vehicle p_{n+1} undergoes the same setpoint change $\zeta_{n+1} = \zeta_n$. Therefore, its headway error is

$$e_{n+1,h}(s) = (G(s) + 1)\zeta_n. \tag{37}$$

Clearly, the disturbance at vehicle p_{n+1} is greater than the one at p_n. This means that, even though the vehicle following controller is string-stable, if all platoon vehicles adjust their headway setpoint at the same time, vehicles upstream would brake for longer and reduce their speeds to lower values than their leaders. To avoid such an undesired effect, we propose to distribute the disturbances over time: p_n only changes its setpoint once vehicle p_{n-1} is back at steady-state. The trade-off is that we change one high impact adjustment for several ones of smaller magnitude.

7.3.   Lateral Controller

The proposed approach to guarantee maneuver safety first synchronizes vehicles speeds and aligns their positions. Then, while keeping constant velocity, vehicles perform lane change. Therefore at any point in time we have either $\dot{v}_x \approx 0$ or $\dot{v}_y \approx 0$. This decoupling of longitudinal and lateral movements allows the lateral dynamics to be described by a linear bicycle model:

$$\frac{\mathrm{d}}{\mathrm{d}t} \begin{bmatrix} y \\ v_y \\ \theta \\ \dot{\theta} \end{bmatrix} = \begin{bmatrix} 0 & 1 & 0 & 0 \\ 0 & -\frac{a_1}{v_x} & 0 & -v_x - \frac{a_2}{v_x} \\ 0 & 0 & 0 & 1 \\ 0 & -\frac{a_3}{v_x} & 0 & -\frac{a_4}{v_x} \end{bmatrix} \begin{bmatrix} y \\ v_y \\ \theta \\ \dot{\theta} \end{bmatrix} + \begin{bmatrix} 0 \\ b_1 \\ 0 \\ b_2 \end{bmatrix} \delta \tag{38}$$

where y, v_y and v_x are, respectively, lateral displacement, lateral velocity and longitudinal velocity based on the vehicle's body coordinates, and θ is its orientation with respect to the road longitudinal axis. The coefficients are:

$$a_1 = 2\frac{C_f + C_r}{m},$$
$$a_2 = 2\frac{C_f l_f - C_r l_r}{m}, \qquad b_1 = 2\frac{C_f}{m},$$
$$a_3 = 2\frac{C_f l_f - C_r l_r}{I_z}, \qquad b_2 = 2\frac{C_f l_f}{I_z}$$
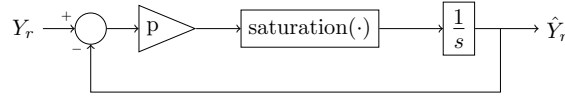$$a_4 = 2\frac{C_f l_f^2 + C_r l_r^2}{I_z},$$

Figure 22: Y_r filter to create smooth transition.

where C_f and C_r are, respectively, front and rear tire cornering stiffness, l_f and l_r are distances from front and rear tires, respectively, to the center of gravity, m is vehicle's mass, and I_z is its yaw moment of inertia. To define the lateral controller, we write out velocities in road coordinates under small angle assumption:

$$\dot{X} = v_x \cos\theta - v_y \sin\theta = v_x - v_y\theta \tag{39}$$

$$\dot{Y} = v_x \sin\theta + v_y \cos\theta = v_x\theta + v_y, \tag{40}$$

where X and Y are longitudinal and lateral coordinates, respectively, in the road's frame of reference. The final model is:

$$\dot{q} = A(v_x)q + B\delta \tag{41}$$

where

$$q = \begin{bmatrix} Y & v_y & \theta & \dot{\theta} \end{bmatrix}^T$$

$$A(v_x) = \begin{bmatrix} 0 & 1 & v_x & 0 \\ 0 & -\frac{a_1}{v_x} & 0 & -v_x - \frac{a_2}{v_x} \\ 0 & 0 & 0 & 1 \\ 0 & -\frac{a_3}{v_x} & 0 & -\frac{a_4}{v_x} \end{bmatrix}$$

$$B = \begin{bmatrix} 0 & b_1 & 0 & b_2 \end{bmatrix}^T.$$

Before the lane change $Y(t_0) = Y_0$, where Y_0 is the center of the origin lane. The reference for lane change is $Y_r = Y_0 + \kappa H$, where $\kappa \in \{+1, -1\}$ defines whether the vehicle moves to the left or right lane respectively, and H is the lane's width. Moreover, after the maneuver it is also required that $[v_y, \theta, \dot{\theta}] = [0, 0, 0]$. The error and its dynamics are therefore

$$e_y = \begin{bmatrix} Y_r - Y & -v_y & -\theta & -\dot{\theta} \end{bmatrix}^T, \tag{42}$$

$$\dot{e}_y = A(v_x)e_y + B\delta. \tag{43}$$

Thus, a state feedback controller $\delta = Ke$ can be used to asymptotically track the new reference. To avoid discontinuities in e, which would cause large and uncomfortable values of δ, we pass Y_r through a low-pass filter as the one used in [42]. It is described by Fig. 22.

Last, we need to address the fact that not all states of e can be measured directly. The lateral position error $Y_r - Y$ can be obtained using a camera and the lane markers. The yaw rate $\dot{\theta}$ is directly measured by the vehicle's gyroscope. Using these two measurements, we can use an

observer to estimate the other states.

8   Simulation Testing and Evaluation

In this section, we use simulation tools to analyze the traffic impacts of the proposed methods. First, we make use of Simulink to verify the proper behavior of the longitudinal and lateral controllers presented in section 7. These simulations also provide metrics to compare the platoon lane change strategies efficiency. Then, to evaluate the traffic impact on the road network and on the environment, we present results obtained using the microscopic simulation software VISSIM.

8.1.   Vehicle Level Simulations

To verify controller behavior and estimate its impacts, we use the simulation software Simulink. It provides a vehicle model block and allows detailed implementation of the control algorithms. We use these capabilities to simulate connected autonomous vehicles and to create the hardest-to-merge scenario. In it, both lanes are assumed to be at full capacity. This entails that vehicles on the same lane have the same initial speed, $v_o(0)$ at the origin lane and $v_d(0)$ at the destination lane. It also implies that all vehicles are keeping minimum vehicle following distances to their respective leaders until t_0. Moreover, in all analyzed scenarios:

- There are a three-vehicle platoon and four surrounding vehicles;

- All vehicles are passenger vehicles with parameters defined in table 1;

- The longitudinal adjustments phase starts at $t_0 = 5s$ and, at this time instant, the vehicle negotiating the lane change is one meter closer to its virtual leader than to its real leader. Mathematically, $g_{p_n,L_d}(t_0) = g_{p_n,L_o}(t_0) - 1$, where $n = 1$ for strategies Synchronous and Leader First, and $n = 3$ for strategy Last Vehicle First.

The initial relative velocity between lanes is defined as:

$$\Delta v_\ell = v_d(0) - v_o(0). \tag{44}$$

We analyze a total of nine scenarios. For each of the three platoon lane changing strategies, there are three possible initial relative velocities $\Delta v_\ell = 0$, $\Delta v_\ell = -14.4 km/h$ and $\Delta v_\ell = 14.4 km/h$. We first present the vehicles' trajectories and errors to verify the platoon lane changing strategies work as intended and to confirm they comply with the safety criteria. Next, the efficiency metrics used to compare the strategies are defined. Last, we the values of these metrics for each strategy.

8.1.1.   Intended Behavior and Safety

In this section, three scenarios are selected to show the proper lane change phases over time and to confirm the safety criteria is met at all times. Each experiment differs both in lane change strategy and in relative velocity between origin and destination lane.
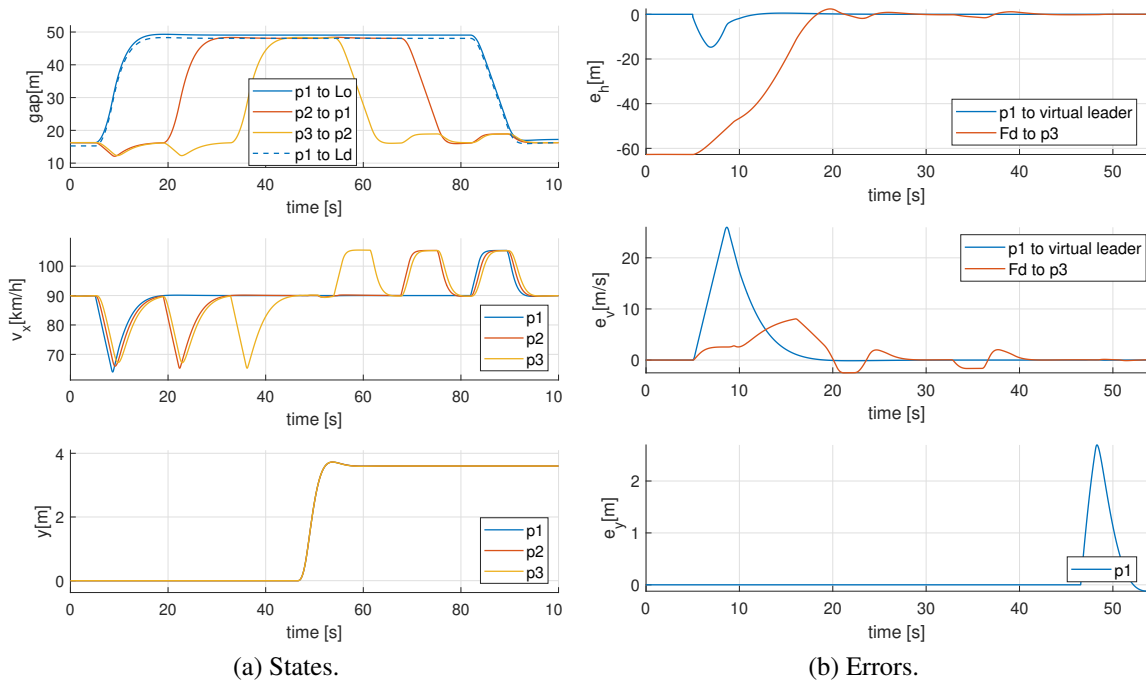
(a) States.

(b) Errors.

Figure 23: Vehicle states (a) and relevant errors (b) for platoon lane change with the Synchronous strategy and zero initial relative velocity between lanes. Plots on the left from top to bottom show inter-vehicle gaps, longitudinal velocity and lateral position. Plots on the right from top to bottom show headway, velocity and lateral errors.

The plots in Fig. 23a allow us to verify correct behavior in the case of **Synchronous Strategy** and $\Delta\mathbf{v}_\ell = \mathbf{0}$. The top plot shows the staggered longitudinal adjustment phase. At the start, all platoon vehicles keep the minimum vehicle following distance $g_{i,j}^{\mathrm{f}}$ to their respective leaders. Then, one by one, they increase this distance to $g_{i,j}^{\mathrm{lc}}$. Vehicle p_1 creates a slightly larger than necessary gap to L_o in order to achieve the desired distance to L_d. The middle plot shows the velocities which cause the gap variation. The lateral movement phase can be identified in the bottom plot. It shows that all vehicles perform the lane change simultaneously, which is the defining characteristic of this strategy. After the lane change, at about $t > 55s$, the gap closing phase starts and platoon vehicles, starting by the last, sequentially decrease the gaps to their leader back to $g_{i,j}^{\mathrm{f}}$. The compliance to safety criteria is better checked in the plots of Fig. 23b. We choose to show error values only up to around $t = t_{\mathrm{lc}}$, when the lateral movement for the entire platoon is completed. After that, real leaders for p_1 and F_d change which make the plots harder to interpret without bringing any gains to the safety analysis. The top two plots present the most relevant headway and velocity errors and the bottom plot shows lateral errors. In this scenario, the critical errors are between p_1 and its virtual leader L_d and between F_d and p_3. The bottom plot confirms that the new reference Y_r, which causes e_y to become positive, is only passed to the vehicles once all headway and velocity errors are non-negative.

The next scenario uses the **Leader First strategy** and $\Delta\mathbf{v}_\ell = -14.4\mathrm{km/h}$, that is, vehicles
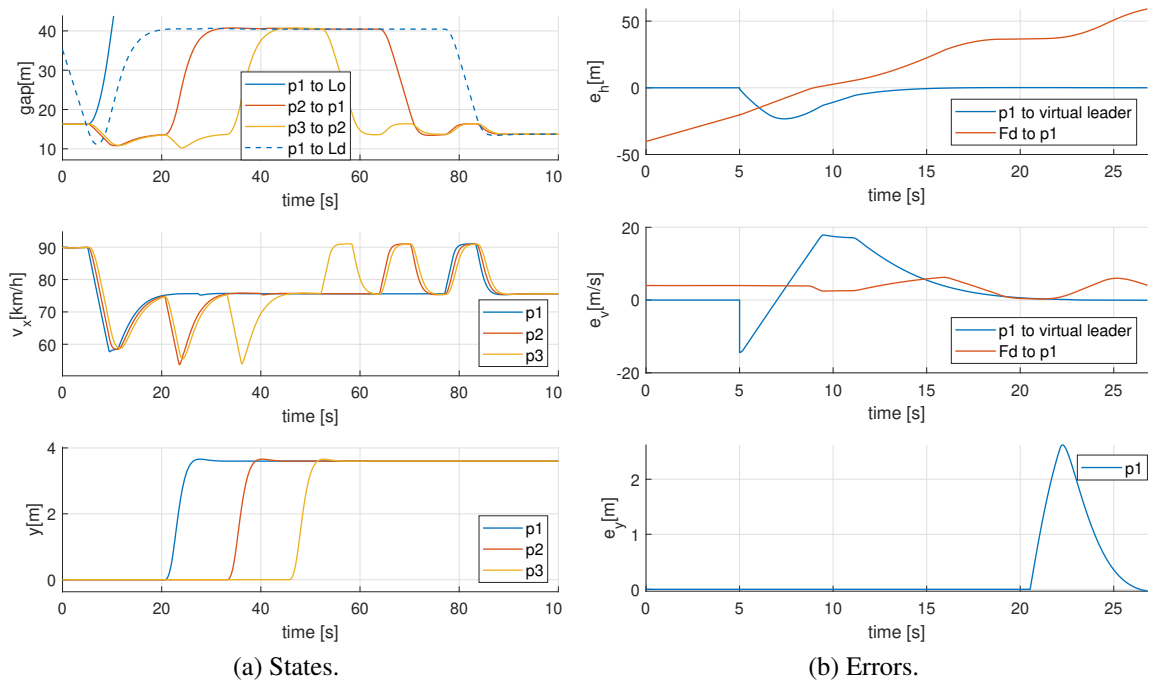
(a) States. (b) Errors.

Figure 24: Vehicle states (a) and relevant errors (b) for platoon lane change with the Leader First strategy and negative initial relative velocity between lanes. Plots on the left from top to bottom show inter-vehicle gaps, longitudinal velocity and lateral position. Plots on the right from top to bottom show headway, velocity and lateral errors.

are merging into a slower lane. The plots in 24a confirm the desired behavior for this strategy. The safe lane change gaps are created similarly to the previous case. The difference now is that the platoon has to slow down first, therefore the gap from p_1 to its leader in the original lane L_o grows quickly. It goes off the chart at about $t = 10s$. In the velocity plot at the middle, one can check that the platoon synchronized its speed to the adjacent lane. At the bottom plot, the Leader First strategy is clearly visible: vehicles start their lateral movements as soon as they individually arrive at steady-state. We present confirmation of safety criteria for vehicle p_1 with the plot of relevant errors in Fig. 24b. Again, only the time up to around $t = t_{lc}$ is show. It is easy to verify that headway and velocity errors (top and middle plots respectively) from p_1 to L_d and from F_d to p_1 are non-negative when the lane change command is given. Vehicle p_1's real leader, L_o is not a concern for p_1's safety because it is traveling at a higher speed and thus distances itself quickly. The headway error between F_d and p_1 keeps increasing because F_d is still creating a gap for the whole platoon. Errors for the other two platoon vehicles follow similar behavior.

Last, we analyze a scenario with the **Last Vehicle First strategy** and $\Delta v_\ell = 14.4km/h$, that is, the platoon is merging into a faster lane. Starting with the plots in Fig. 25a, the gap plot at the top is quite different from the previous two ones because the last platoon vehicle p_3 starts the longitudinal adjustments phase first. Another two points to notice in this plot. First, the gap between p_3 and the leader at the destination lane L_d increases quickly and goes off the chart at
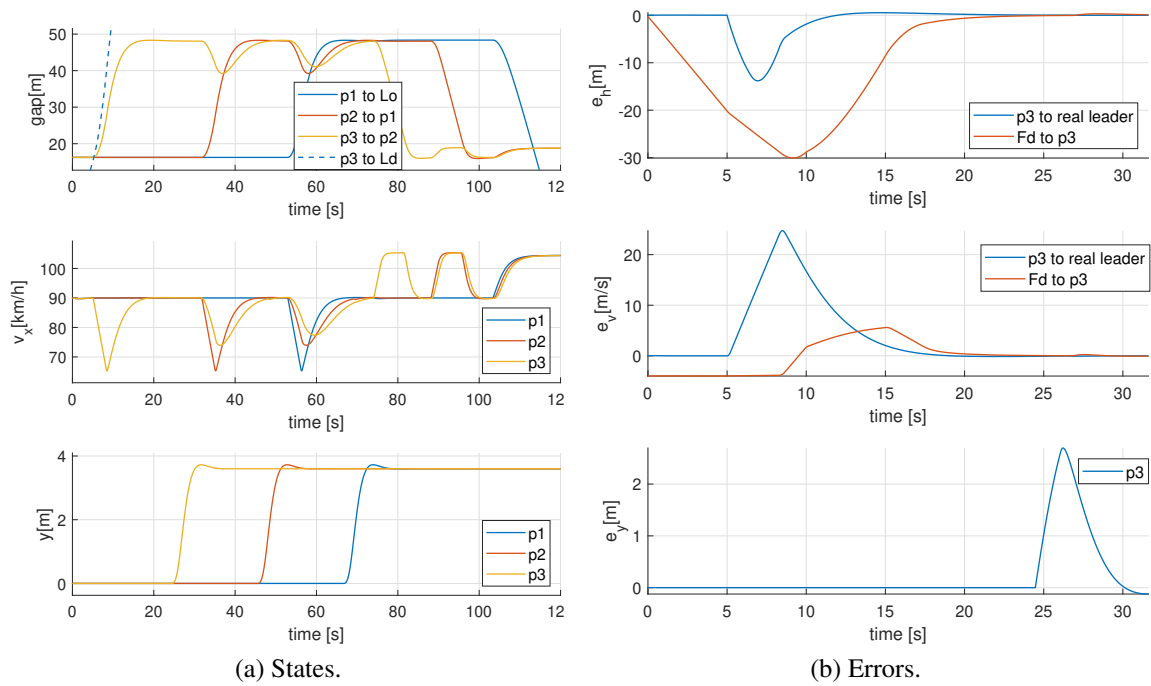
Figure 25: Vehicle states (a) and relevant errors (b) for platoon lane change with the Last Vehicle First strategy and positive initial relative velocity between lanes. Plots on the left from top to bottom show inter-vehicle gaps, longitudinal velocity and lateral position. Plots on the right from top to bottom show headway, velocity and lateral errors.

about $t = 10s$ because this vehicle is traveling faster than the platoon. Second, we notice that the gap from p_1 to L_o decreases sharply towards the end of the maneuver. This happens because, once the lane change is completed, platoon vehicles accelerate to match the speed at their new lane, as confirmed by the velocity plot at the middle. The other noticeable difference from this strategy is made evident by the bottom plot, where the lateral movement phases start from last to first platoon vehicle. Maneuver safety regarding p_3 is confirmed by the relevant error plots in Fig. 25b. With positive relative velocity between lanes, the virtual leader L_d distances itself quickly and is therefore not a concern for p_3's safety. The top and middle plots confirm that headway and velocity errors are positive by the time p_3 is allowed to start its lateral movement. Errors for p_2 and p_1 are similar.

8.1.2. Metrics

Before moving on to results on efficiency, we need to define the three metrics used to evaluate it. They are:

Maneuver Duration
This metric is mathematically defined as:

$$T = t_f - t_0. \tag{45}$$

Reserved Space-Time

We need a metric to express road sub-utilization during the maneuver. In [36], maneuver efficiency is measured by the space-time that it occupies, which is defined as the integral of space over time. For our purposes, we want to compute the integral of *reserved unoccupied* space $r_k(t)$ in front of each vehicle k. Reserved unoccupied space is defined such that $r_k(t) = 0$ during regular vehicle following with minimum safe gap:

$$r_k(t) = f_k(t) - (x_k(t) + g^{\text{f}}_{k,k-1}(t)) \qquad (46)$$

where $f_k(t)$ is the longitudinal coordinate of the end of the free space ahead of vehicle k, $x_k(t)$ is vehicle k's front bumper longitudinal coordinate, and $g^{\text{f}}_{k,k-1}(t)$ is the minimum safe vehicle following gap between k and its real leader. In some cases, $f_k(t) = x_{k-1}(t)$, that is, the free space is determined by the position of the preceding vehicle. The values of $r_{F_d}(t)$ and $r_{p_2}(t)$ in Fig. 26a and of $r_{F_d}(t)$ in Fig. 26b are computed this way. In other cases, $r_k(t)$ depends on the safe lane changing distances. For example, in Fig. 26b, after p_1 has changed lanes, the gap from p_2 to L_o is bigger than necessary for p_2's lane change. All the additional space greater than $g^{\text{lc}}_{p_2,L_o}$ ahead of p_2 is not reserved and thus does not add to $r_{p_2}(t)$. A similar situation occurs when one lane is traveling faster than the other. In Fig. 26c, the destination lane's velocity is higher than the origin lane's. While F_d is creating a gap for p_N, L_d is "getting away". Once again, part of the free space between F_d and L_d is not reserved for the maneuver and is not counted when computing $r_{F_d}(t)$. The analysis for the scenario where the origin lane is faster is similar. The final total space-time cost is:

$$R = \sum_{k=\{F_d, p_1, \ldots, p_N\}} \int_{t_0}^{t_f} r_k(t)\mathrm{d}t \qquad (47)$$

Acceleration costs

Another interesting metric is the total control effort during the maneuver:

$$U = \sum_{k=\{F_d, p_1, \ldots, p_N\}} \int_{t_0}^{t_f} a_k^2(t)\mathrm{d}t \qquad (48)$$

where a_k is the acceleration of vehicle k. This metric is usually associated with fuel consumption and passenger comfort.

8.1.3. Efficiency

The values of the proposed metrics for each of the nine experiments is presented in table 4. The abbreviations *Sync.*, *Ld. F.* and *L.V.F.* on the strategy column stand for Synchronous, Leader First and Last Vehicle First respectively. Regarding maneuver duration and acceleration cost, strategies Synchronous and Leader First present no significant differences. However, when it comes to reserved space-time, the Leader First strategy shows an improvement of at least 20% for all relative speeds. By allowing vehicles to move in one by one, this approach frees space in the origin lane and occupies the reserved space in the destination lane faster. The Last Vehicle First strategy contrasts
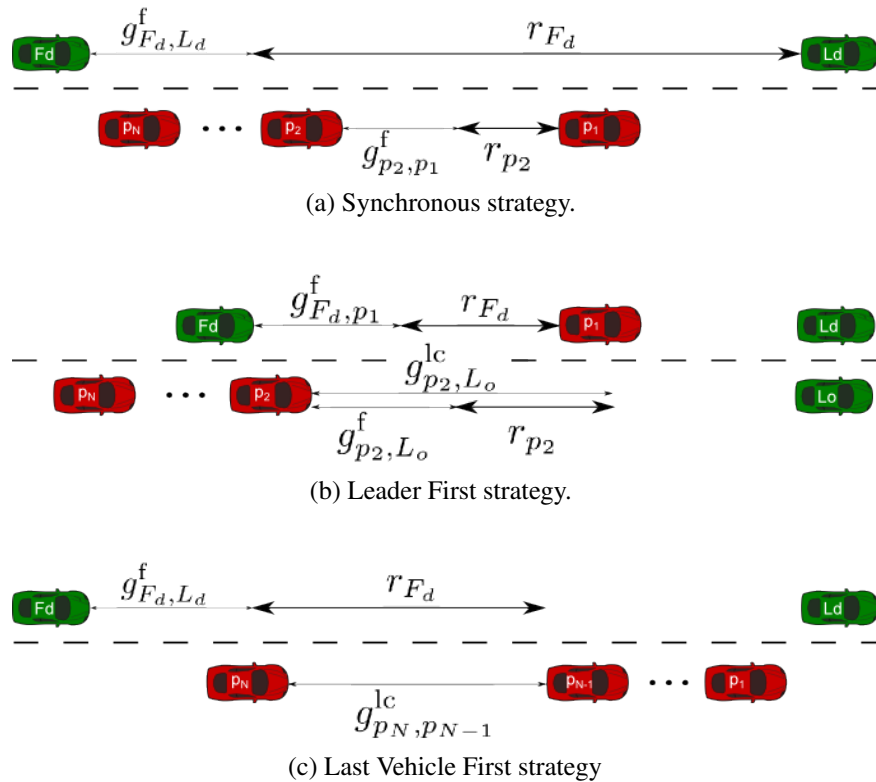
(a) Synchronous strategy.

(b) Leader First strategy.

(c) Last Vehicle First strategy

Figure 26: Examples of reserved space $r_k(t)$ for different vehicles and in different traffic configurations.

Table 4: Efficiency Results.

$\Delta v_L(km/h)$	Strategy	Maneuver Duration (s)	Acceleration Cost (m^2/s^3)	Reserved Space-Time $(m.s)$
0	Sync.	91	359	10234
	Ld. F.	91	367	8026
	L.V.F.	114	321	9237
-14.4	Sync.	86	327	8089
	Ld. F.	85	326	6388
	L.V.F.	N/A	N/A	N/A
14.4	Sync.	85	299	8826
	Ld. F.	85	305	5750
	L.V.F.	98	209	7810

more clearly with the previous two. It is the one which takes the longest to complete, not being able to finish within 2 minutes for the case of negative relative velocity. On the other hand, because it forces F_d to decelerate less, this strategy obtains the best acceleration costs. When it comes to reserved space-time, the smaller impact on F_d and the longer total maneuver time make this strat-
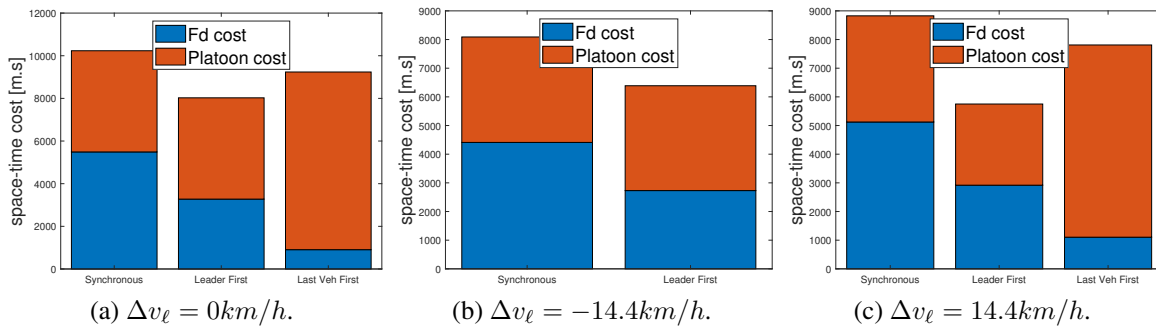
(a) $\Delta v_\ell = 0 km/h.$ (b) $\Delta v_\ell = -14.4 km/h.$ (c) $\Delta v_\ell = 14.4 km/h.$

Figure 27: Reserved space-time costs for each relative velocity and each strategy. The costs are shown separately for F_d in blue and for the platoon vehicles in orange.

egy perform somewhere between the other two. To study reserved space-time more deeply, Fig. 27 shows the how much of the cost comes from empty space ahead of F_d and how much comes from the platoon. The platoon share includes unoccupied space ahead of p_1 as well as extra gaps between platoon vehicles. As expected, the Last Vehicle First strategy has the smallest share of reserved space in front of F_d. The other two strategies have almost the same platoon cost but Leader First has much smaller F_d cost.

The optimum lane change trajectory for moving into a slower lane is given by the Leader First strategy. For non-negative relative speeds, the choice depends on the system designer objectives. While the Leader First strategy finishes faster and with considerably lower reserved space-time, the Last Vehicle First yields better acceleration costs. Furthermore, we should remember that F_d is the vehicle actively cooperating to generate a gap for others. If one wants to favor a strategy that minimally impacts F_d, the Last Vehicle First is the best choice.

8.2. Microscopic Simulations

To further evaluate the impact of the proposed methods, we use the commercial microsimulation software VISSIM. Whereas the previous experiments in Simulink allowed the detailed control of a small set of vehicles in simplified well-behaved settings, VISSIM supports simulations of thousands of vehicles and their interactions in realistic scenarios. Each vehicle is an agent with built-in vehicle following and lane changing models. At each simulation time step, the vehicle feeds these models with information about its states and its environment to determine its behavior. Vehicle parameters, such as length and maximum speed, as well as driver parameters such as thresholds for increasing or decreasing following distances, can be set by the user. Moreover, VISSIM uses stochastic distributions of speed and spacing thresholds to better depict the variability of human behavior.

Thanks to these capabilities, it is possible to extract commonly used traffic measurements from the simulations. We choose to evaluate the proposed methodologies impacts on traffic flow by two

metrics. To assess our method's efficiency, we use mean travel time:

$$\bar{T}_t = \frac{1}{N} \sum_{n=1}^{N} t_{\text{out},n} - t_{\text{in},n} \tag{49}$$

where N is the total number of vehicles that pass a certain region of the highway and $t_{\text{out},n}$ and $t_{\text{in},n}$ represent the time instants vehicle n exits and enters the simulation respectively. To estimate the method's impact on safety, we use mean number of stops

$$\bar{s} = \frac{1}{N} \sum_{n=1}^{N} s_n, \tag{50}$$

where s_n counts how many times vehicle n stopped. Lower values of $\bar{s}$ are associated with smoother traffic flow and smaller crash probability.

The impacts on the environment are gauged by average fuel consumption rate and average CO_2, NO_x and PM25 emission rates over distance traveled. Mathematically,

$$R = \frac{\sum_{n=1}^{N} E_n}{\sum_{n=1}^{N} d_n}, \tag{51}$$

where E_n stands for vehicle n's fuel consumption or emission of any of the pollutants and d_n is the distance traveled by the same vehicle. The values of E_n are estimated by the MOVES model. From the Environment Protection Agency's (EPA) website, "EPA's MOtor Vehicle Emission Simulator (MOVES) is a state-of-the-science emission modeling system that estimates emissions for mobile sources at the national, county, and project level for criteria air pollutants, greenhouse gases, and air toxics".

8.2.1.   Set-up

Since VISSIM creates realistic traffic situations, it is not possible to reproduce the exact full occupancy conditions of previous Simulink simulations. Therefore, we must first describe how to create a relevant scenario in VISSIM.

The experiments take place on a 16km-long south-bound stretch of the I-710 California highway as shown in Fig. 28. A VISSIM model of this segment was created and calibrated using historical data. To evaluate the effectiveness of the proposed methods, we want a scenario where lane changes occur often in a vehicle-dense environment. To obtain these conditions, an incident that closes the middle lane of a segment with three lanes is created at the location marked by a red dot in Fig. 28. With this, the maximum theoretical vehicle capacity drops from around 8400 veh/h to around 5600 veh/h. Moreover, to force a high number of lane changes, the simulated vehicle demand is set to be higher than the bottleneck capacity.

The next step is to make vehicles in the simulation behave according to the proposed control algorithms. VISSIM's built-in driver model does not account for connectivity, which means they

Pacific Southwest Region UTC
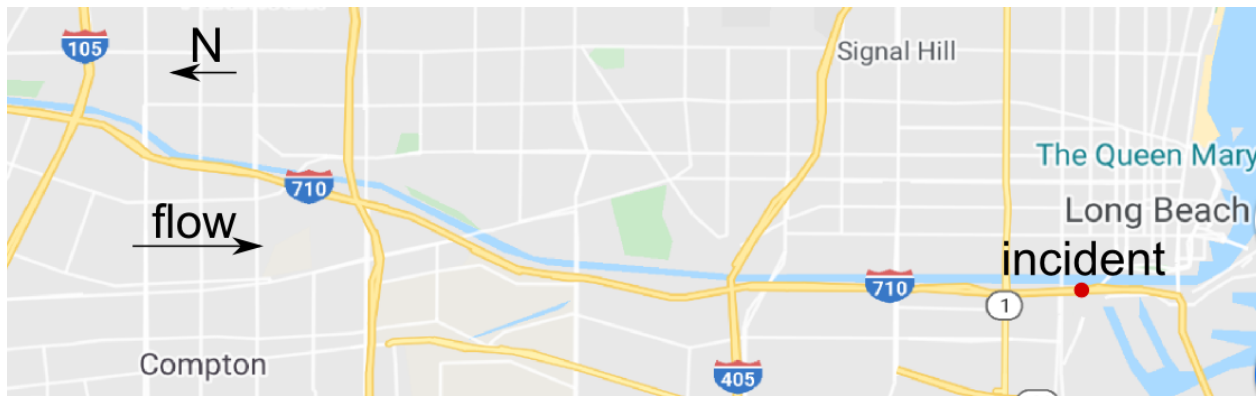University Transportation Center

Figure 28: I-710 highway segment used for experiments.

cannot follow the communication protocol for gap generation or travel close together as platoons. Even though these limitations originate from the same issue, they are addressed separately. To emulate the behavior of the gap generating controllers, two VISSIM features are used together: lane change recommendation and speed limits. The lane change recommendation sign is created about a kilometer upstream the incident location. This serves two objectives. First, it allows vehicles to know beforehand about the lane closure ahead (as would happen in a connected environment) giving them time to look for appropriate naturally occurring lane change gaps on adjacent lanes. Since the simulation parameters create a dense vehicle area, such spacings are not easily found. Thus, the recommendation upstream of the accident also provides the equivalent necessary time for vehicles to communicate requesting gaps. Then, the speed limits, which are also added to sections upstream the incident, play the role of mimicking the gap generation controller. These limits are given to vehicles at approximately every 500m interval starting about 5km upstream of the accident. Moreover, two consecutive limits do not differ by more than 5mi/h to allow smooth adaptation and their lower and upper boundaries are 10mi/h and 65mi/h respectively. This produces the effect of vehicles in the destination lane slowing down to create spacings for those which intend to change lanes. The approach to consider the effect of platoons is to include trucks in the simulation. Since trucks are longer, they consume more fuel and require larger gaps to merge, as do platoons.

8.2.2.   Road-Level Results

For the results presented here, the lane closure only starts after 5 minutes of simulation. This avoids corrupting the measurements with transient behavior at start-up. In addition, the incident remains in place until the simulation ends, which takes another 40 minutes. The chosen demands are 6000 veh/h and 6500 veh/h with 15% of platoons. To decrease sensibility due to the randomness of VISSIM simulations, all presented values are the average of 10 sets of Monte Carlo runs with different seeds. The results presented in Table 5 show the advantages of the proposed approach. Without any control, the bottleneck with high vehicle density creates the inefficient and unsafe situation where a vehicle stuck behind the closure has close to zero velocity and must merge into

Table 5: VISSIM Simulation Results.

	6000 veh/h			6500 veh/h		
	No Control	Control	Improvement	No Control	Control	Improvement
$T_t(s)$	19.84	16.69	-15.89%	21.25	16.55	-22.13%
$\bar{s}$	15.46	1.74	-88.75%	16.12	1.83	-88.65%
Energy (kJ/mi)	182.55	169.39	-7.21%	182.85	168.11	-8.06%
CO_2 (g/mi)	570.72	529.76	-7.18%	568.96	523.25	-8.04%
NO_x (g/mi)	1.58	1.50	-4.95%	1.58	1.50	-4.95%
PM25 (g/mi)	0.052	0.050	-3.74%	0.052	0.050	-3.74%

a fast speed adjacent lane. This causes the lane changing vehicle to wait considerably for a proper gap and creates a queue on that lane. Furthermore, it forces vehicles in the destination lane to slow significantly and in a short time interval to avoid accidents when lane changes take place in front of them. Such a behavior yields an elevated number of stops. Not surprisingly, the value $\bar{s}$ presents the greatest decrease once control is applied. Not only that, thanks to a smoother traffic flow, the total travel time $\bar{T}_t$ also decreases substantially. Improving these two metrics has a direct effect on the environmental impact. The relative gains in fuel consumption and CO_2 emissions are nearly the same since carbon dioxide is the main byproduct of fuel combustion. The other two measured pollutant emissions are also lowered.

8.3. Lane-Level Results

To deepen our understanding of the controller effects on the scenario, we analyze what happens on each lane as a function of the vehicle demand. The variables that best describe the state of traffic flow on a lane are vehicle density and flow-rate. The first, henceforth called ρ, is measured in vehicles per mile (per lane) and it represents how tightly packed are vehicles on a certain segment of the lane. The second, q from here on, measures how many vehicles pass by that lane segment within a time interval and its typical unit is vehicles per hour (per lane). The relationship between these variables has been shown to follow what is commonly known as the triangular fundamental diagram [43]. Fig. 29 illustrates what a typical fundamental diagram looks like for a road section. While this shape is obtained from rigorous math, for our purposes we can proceed with an intuitive understanding of it. The first part of the diagram, with positive slope, represents an uncongested situation, where an increase in density means an increase in flow. However, roads have limited capacity, denoted C in the diagram. After the corresponding critical density ρ^c, the road is in a congested state, where higher densities imply lower flows. One can easily visualize this in a busy highway during rush-hour: when vehicles are all bumper to bumper, the density is elevated but the flow is considerably low.

To evaluate the effects of the lane change controller, the same previously described scenario is used, but now traffic demand is varied over a wide range of values. It is useful to note that the capacity per lane is estimated at around 2800 veh/h before the incident happens. Density
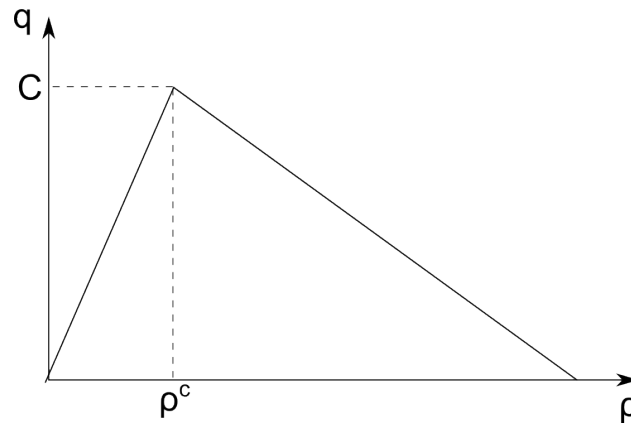
Figure 29: Example of typical fundamental diagram.

(a) Fundamental diagram of lane 1
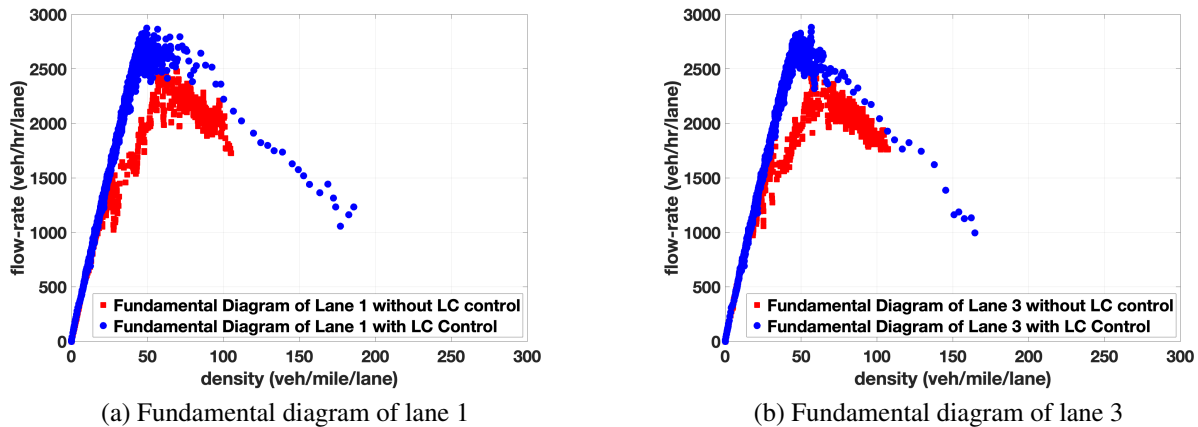

(b) Fundamental diagram of lane 3

Figure 30: Fundamental diagrams with (blue) and without (red) lane change control for the remaining open lanes.

and flow at the open lanes (first and third) at the segment immediately upstream of the incident are measured in simulations both with and without control. Results are shown in Fig. 30, where red squares indicate the measurements without control and blue circles the ones with control. It's visible that both lanes are equally affected by the closure of the middle lane and they achieve a maximum flow of approximately 2400 veh/h in the case without control. This is due to the previously explained behavior of slow vehicles having to force themselves in the faster adjacent lanes. On the other hand, the flow goes up to around 2800 veh/h in the scenario with controller showing that maximum capacity is again achieved despite the incident. We conclude that the proposed methods can increase traffic flow efficiency.

9 Conclusion

In this work, we studied several challenges concerning safe autonomous lane changes in congested scenarios. Our solution to address safety and efficiency simultaneously is based on vehicle communication and cooperation. The first step was to define what constitutes a safe gap for lane changing. Besides relying on previous results of safe vehicle following and lane change kinematics, we make a conservative assumption to define a constant maximum braking during lane change. The main advantage of this method is seen later on when this larger spacing request is seamlessly included in the longitudinal vehicle controller. Concerning communication, we proposed a protocol that details what information vehicles should exchange and how to avoid conflicts. After reviewing works on the DSRC standard and its performance, we conclude that our protocol can be implemented. We also analyze how to expand safety spacing requirements and communications to platoons of vehicles. Our solution is based on three strategies, Synchronous, Leader First and Last Vehicle First, which can ensure the platoon remains together after the lane change. Next, we examined how to make use of physical and analytical redundancies to verify the requested gaps are indeed created. The proposed methodology compares several measurements and internal model predictions to check for consistency and identify possible system faults. It also defines the severity of each failure and when the driver is asked to take control. Then, we developed control policies that enable lane changes in the most congested scenarios while satisfying the strict safety requirements. Thanks to communications, vehicles with the intention to change lanes as well as the one responsible for creating the gap can adopt a virtual leader. They keep using the preceding vehicle on their own lanes as the real leader for safety purposes while the virtual leader makes them longitudinally adjust themselves for the maneuver. We showed how this can be achieved with two parallel constant time headway controllers through simulations. Moreover, these experiments allowed us to compare the efficiency of the three proposed platoon strategies. We establish that the Leader First strategy is, on average, the best. However, the Last Vehicle First option is advantageous if one wants to minimize the discomfort of the vehicle creating the gap. After confirming the expected behavior from controllers, VISSIM simulations are used to assess impacts on traffic flow and the environment. The microscopic simulation scenario set-up is explained and its results indicate that the developed methods improve both safety and efficiency. With no control, vehicles queue waiting for a proper lane change space and, when they find one, they force large decelerations on the destination lane. With control, the traffic flow gets smoother since vehicles are able to perform lane changes before being forced to a full stop. This decreases the number of stops and the total travel time. Consequentially, fuel consumption and pollutant emission rates are also lowered. The gains in efficiency are corroborated by a deeper study of individual lanes' densities and flows. The fundamental diagrams show improved traffic flow in the simulations with control.

10   References

[1] T. Reed and J. Kidd, "Global Traffic Scorecard," Tech. Rep. February, 2019.

[2] National Highway Traffic Safety Administration, "2017 Fatal Motor Vehicle Crashes: Overview," no. October, 2018.

[3] A. Talebpour and H. S. Mahmassani, "Influence of connected and autonomous vehicles on traffic flow stability and throughput," *Transportation Research Part C: Emerging Technologies*, vol. 71, pp. 143–163, 2016.

[4] H. S. Mahmassani, "50th Anniversary Invited Article—Autonomous Vehicles and Connected Vehicle Systems: Flow and Operations Considerations," *Transportation Science*, vol. 50, no. 4, pp. 1140–1162, 2016.

[5] P. A. Ioannou and C. C. Chien, "Autonomous Intelligent Cruise Control," *IEEE Transactions on Vehicular Technology*, vol. 42, no. 4, pp. 657–672, 1993.

[6] A. Kanaris, P. Ioannou, and F.-s. Ho, "Spacing and Capacity Evaluations for different AHS Concepts," Tech. Rep., 1995.

[7] M. Rahman, M. Chowdhury, Y. Xie, and Y. He, "Review of microscopic lane-changing models and future research opportunities," *IEEE Transactions on Intelligent Transportation Systems*, vol. 14, no. 4, pp. 1942–1956, 2013.

[8] H. Jula, E. B. Kosmatopoulos, and P. A. Ioannou, "Collision avoidance analysis for lane changing and merging," *IEEE Transactions on Vehicular Technology*, vol. 49, no. 6, pp. 2295–2308, 2000.

[9] A. Kanaris, E. B. Kosmatopoulos, and P. A. Ioannou, "Strategies and spacing requirements for lane changing and merging in automated highway systems," *IEEE Transactions on Vehicular Technology*, vol. 50, no. 6, pp. 1568–1581, 2001.

[10] Y. Luo, G. Yang, M. Xu, Z. Qin, and K. Li, "Cooperative Lane-Change Maneuver for Multiple Automated Vehicles on a Highway," *Automotive Innovation*, vol. 2, no. 3, pp. 157–168, 2019.

[11] C. Hatipoglu, Ü. Özguner, and K. A. Redmill, "Automated lane change controller design," *IEEE Transactions on Intelligent Transportation Systems*, vol. 4, no. 1, pp. 13–22, 2003.

[12] H. Yu, H. E. Tseng, and R. Langari, "A human-like game theory-based controller for automatic lane changing," *Transportation Research Part C: Emerging Technologies*, vol. 88, no. February, pp. 140–158, 2018.

[13] D. Ni, J. Li, S. Andrews, and H. Wang, "A methodology to estimate capacity impact due to connected vehicle technology," *International Journal of Vehicular Technology*, vol. 2012, 2012.

[14] B. Van Arem, C. J. G. Van Driel, and R. Visser, "The impact of cooperative adaptive cruise control on traffic-flow characteristics," *IEEE Transactions on Intelligent Transportation Systems*, vol. 7, no. 4, pp. 429–436, 2006.

[15] P. G. Gipps, "A model for the structure of lane-changing decisions," *Transportation Research Part B*, vol. 20, no. 5, pp. 403–414, 1986.

[16] T. Toledo, C. Choudhury, and M. Ben-Akiva, "Lane-Changing Model with Explicit Target Lane Choice," *Transportation Research Record: Journal of the Transportation Research Board*, vol. 1934, no. Lane 3, pp. 157–165, 2005.

[17] A. Talebpour, H. S. Mahmassani, and S. H. Hamdar, "Modeling Lane-Changing Behavior in a Connected Environment: A Game Theory Approach," *Transportation Research Procedia*, vol. 7, pp. 420–440, 2015.

[18] Z. Huang, D. Chu, C. Wu, and Y. He, "Path Planning and Cooperative Control for Automated Vehicle Platoon Using Hybrid Automata," *IEEE Transactions on Intelligent Transportation Systems*, pp. 1–16, 2018.

[19] H. C.-h. H. Hsu and A. Liu, "Kinematic design for platoon-lane-change maneuvers," *IEEE Transactions on Intelligent Transportation Systems*, vol. 9, no. 1, pp. 185–190, 2008.

[20] M. Xu, Y. Luo, G. Yang, W. Kong, and K. Li, "Dynamic Cooperative Automated Lane-Change Maneuver Based on Minimum Safety Spacing Model *," *2019 IEEE Intelligent Transportation Systems Conference (ITSC)*, pp. 1537–1544, 2019.

[21] A. Kesting, M. Treiber, and D. Helbing, "General Lane-Changing Model MOBIL for Car-Following Models," *Transportation Research Record: Journal of the Transportation Research Board*, vol. 1999, no. January, pp. 86–94, jan 2007.

[22] S. Ulbrich and M. Maurer, "Towards Tactical Lane Change Behavior Planning for Automated Vehicles," in *2015 IEEE 18th International Conference on Intelligent Transportation Systems*, vol. 2015-Octob. IEEE, sep 2015, pp. 975–981.

[23] R. Schubert, K. Schulze, and G. Wanielik, "Situation assessment for automatic lane-change maneuvers," *IEEE Transactions on Intelligent Transportation Systems*, vol. 11, no. 3, pp. 607–616, 2010.

[24] A. Pierson, W. Schwarting, S. Karaman, and D. Rus, "Learning Risk Level Set Parameters from Data Sets for Safer Driving," in *Intelligent Vehicles Symposium*, 2019.

[25] J. Nilsson, M. Brannstrom, E. Coelingh, and J. Fredriksson, "Lane Change Maneuvers for Automated Vehicles," *IEEE Transactions on Intelligent Transportation Systems*, vol. 18, no. 5, pp. 1087–1096, 2017.

[26] Y. L. Morgan, "Notes on DSRC & WAVE standards suite: Its architecture, design, and characteristics," *IEEE Communications Surveys and Tutorials*, vol. 12, no. 4, pp. 504–518, 2010.

Pacific
Southwest
Region UTC
University Transportation Center

[27] F. Bai and H. Krishnan, "Reliability Analysis of DSRC Wireless Communication for Vehicle Safety Applications," *IEEE Intelligent Transportation Systems Conference (ITSC)*, pp. 355–362, 2006.

[28] J. Rios-Torres and A. A. Malikopoulos, "A Survey on the Coordination of Connected and Automated Vehicles at Intersections and Merging at Highway On-Ramps," *IEEE Transactions on Intelligent Transportation Systems*, vol. 18, no. 5, pp. 1066–1077, 2017.

[29] A. Uno, T. Sakaguchi, and S. Tsugawa, "A merging control algorithm based on inter-vehicle communication," *Proceedings 199 IEEE/IEEJ/JSAI International Conference on Intelligent Transportation Systems*, pp. 783–787, 1999.

[30] X.-Y. Lu, H.-S. Tan, S. E. Shladover, and J. K. Hedrick, "Automated vehicle merging maneuver implementation for AHS," *Vehicle System Dynamics*, vol. 41, no. 2, pp. 85–107, 2004.

[31] H. Liu, W. Zhuang, G. Yin, Z. Tang, and L. Xu, "Strategy for heterogeneous vehicular platoons merging in automated highway system," *Proceedings of the 30th Chinese Control and Decision Conference, CCDC 2018*, pp. 2736–2740, 2018.

[32] K. Raboy, J. Ma, E. Leslie, F. Zhou, K. Rush, and J. Stark, "A Proof-Of-Concept Field Experiment on Cooperative Control for Lane Change Maneuvers with New Connected and Automated Vehicle Technologies," *Transportation Research Board 96th Annual Meeting*, pp. 1–10, 2017.

[33] Z. H. Khattak, B. L. Smith, H. Park, and M. D. Fontaine, "Cooperative lane control application for fully connected and automated vehicles at multilane freeways," *Transportation Research Part C: Emerging Technologies*, vol. 111, no. November 2019, pp. 294–317, 2020.

[34] E. Semsar-Kazerooni, K. Elferink, J. Ploeg, and H. Nijmeijer, "Multi-objective platoon maneuvering using artificial potential fields," *IFAC-PapersOnLine*, vol. 50, no. 1, pp. 15 006–15 011, 2017.

[35] M. Wang, S. P. Hoogendoorn, W. Daamen, B. van Arem, and R. Happee, "Game theoretic approach for predictive lane-changing and car-following control," *Transportation Research Part C: Emerging Technologies*, vol. 58, pp. 73–92, 2015.

[36] X. Sun, R. Horowitz, and C.-W. Tan, "An Efficient Lane Change Maneuver for Platoons of Vehicles in an Automated Highway System," *Dynamic Systems and Control, Volumes 1 and 2*, vol. 2003, no. 1, pp. 355–362, 2003.

[37] Y. Sun and P. Ioannou, "A Handbook For Inter-vehicle Spacing In Vehicle Following," Tech. Rep., 1995.

[38] B. Mourllion, D. Gruyer, and A. Lambert, "A study on the safety-capacity tradeoff improvement by warning communications," *IEEE Conference on Intelligent Transportation Systems, Proceedings, ITSC*, pp. 993–999, 2006.

Pacific Southwest Region UTC
University Transportation Center

[39] N. S. Johnson and H. C. Gabler, "Accuracy of a Damage-Based Reconstruction Method in NHTSA Side Crash Tests," *Traffic Injury Prevention*, vol. 13, no. 1, pp. 72–80, 2012.

[40] R. Rajamani, *Vehicle Dynamics and Control*, ser. Mechanical Engineering Series.   Boston, MA: Springer US, 2012.

[41] B. Cronin, "Vehicle Based Data and Availability," 2012.

[42] P. A. Ioannou and Z. Xu, "Throttle and Brake Control Systems for Automatic Vehicle Following," *I V H S Journal*, vol. 1, no. 4, pp. 345–377, 1994.

[43] C. F. Daganzo, "The cell transmission model: A dynamic representation of highway traffic consistent with the hydrodynamic theory," *Transportation Research Part B*, vol. 28, no. 4, pp. 269–287, 1994.

11 Data Management Plan

Products of Research

This study did not collect any data. All results are obtained from simulations whose parameters are described in the report.

Data Format and Content

Not applicable.

Data Access and Sharing

Further details about the results obtained in this study can be obtained by contacting the authors at fvallada@usc.edu.

Reuse and Redistribution

The results from this work have no restrictions concerning reuse and redistribution by the general public.

Pacific
Southwest
Region UTC
University Transportation Center